Automatic versus choice-dependent value representations in the human brain

Grueschow, Marcus; Polania, Rafael; Hare, Todd A; Ruff, Christian C

Abstract: The subjective values of choice options can impact on behavior in two fundamentally different types of situations: first, when people explicitly base their actions on such values, and second, when values attract attention despite being irrelevant for current behavior. Here we show with functional magnetic resonance imaging (fMRI) that these two behavioral functions of values are encoded in distinct regions of the human brain. In the medial prefrontal cortex, value-related activity is enhanced when subjective value becomes choice-relevant, and the magnitude of this increase relates directly to the outcome and reliability of the value-based choice. In contrast, activity in the posterior cingulate cortex represents values similarly when they are relevant or irrelevant for the present choice, and the strength of this representation predicts attentional capture by choice-irrelevant values. Our results suggest that distinct components of the brain's valuation network encode value in context-dependent manners that serve fundamentally different behavioral aims.

DOI: https://doi.org/10.1016/j.neuron.2014.12.054

Automatic versus choice-dependent value representations in the human brain

Marcus Grueschow, Rafael Polania, Todd A. Hare and Christian C. Ruff

Laboratory for Social and Neural Systems Research, Dept. of Economics,

University of Zurich, 8006 Zürich, Switzerland

Correspondence to:

- Marcus Grueschow, Department of Economics, University of Zurich, 8006 Zurich, Blümlisalpstrasse 10,

  Tel: +41-446345595,

  e-mail: marcus.grueschow@econ.uzh.ch

- Christian C. Ruff, Department of Economics, University of Zurich, 8006 Zurich, Blümlisalpstrasse 10,

  Tel: +41-446345067,

  e-mail: christian.ruff@econ.uzh.ch

RUNNING TITLE

Automatic vs. choice-dependent value representations

SUMMARY

The subjective values of choice options can impact on behavior in two fundamentally different types of situations: First, when people explicitly base their actions on such values and second, when values attract attention despite being irrelevant for current behavior. Here we show with functional magnetic resonance imaging that these two behavioral functions of values are encoded in distinct regions of the human brain. In the medial prefrontal cortex, value-related activity is enhanced when subjective value becomes choice-relevant and the magnitude of this increase relates directly to the outcome and reliability of the value-based choice. In contrast, activity in the posterior cingulate cortex represents values similarly when they are relevant or irrelevant for the present choice, and the strength of this representation predicts attentional capture by choice-irrelevant values. Our results suggest that distinct components of the brain's valuation network encode value in context-dependent manners that serve fundamentally different behavioral aims.

Highlights

- Value representations in different brain regions serve different behavioral aims
- mPFC value coding is choice-dependent and relates to the outcome and reliability of value-based choices
- PCC value coding is automatic and relates to value-driven attentional capture

INTRODUCTION

Any decision based on personal preferences rests on the subjective value (SV) of the choice options, for example when deciding which food to eat or whether to buy a product at a given price (Kahneman and Tversky, 1979; Rangel et al., 2008). Elucidating the neural mechanisms by which such SVs are represented is therefore paramount for understanding both healthy and maladaptive choice behavior (Bickel et al., 2007; Dixon et al., 2006; Leotti et al., 2010). To address this issue, numerous laboratory studies have correlated SVs during value-based choices with brain activity and have identified a valuation system comprising several regions, including the medial prefrontal cortex (mPFC), the posterior cingulate cortex (PCC) and the ventral striatum (VS) (for recent meta-analyses see Bartra et al., 2013; Clithero and Rangel, 2013). Critically, these studies typically examined value representations during choices in which the goal is to maximize the personal benefit of the agent and which are therefore taken based on the SVs (anticipated rewards and possibly costs) of the choice options. In these situations, participants naturally focus their attention on the choice-relevant SV.

However, there is growing evidence that SVs can also influence behavior when they are currently choice-irrelevant and therefore outside the focus of attention (Della Libera and Chelazzi, 2006; Hickey et al., 2011; Theeuwes and Belopolsky, 2012). More specifically, the presence of a task-irrelevant item that was previously coupled with a reward can slow down performance of purely perceptual decisions performed on non-value-related stimulus dimensions (Anderson, 2013; Awh et al., 2012). This phenomenon – termed value-based attentional capture – is thought to reflect a brain mechanism that constantly monitors the environment for behaviorally relevant stimuli that may warrant a new course of action (Anderson, 2013; Pearson et al., 2011). This

mechanism may allow the agent to notice valuable unattended alternative stimuli and enable behavioral engagement when this is beneficial.

Very little is known about how task-irrelevant SVs are represented in the brain and how they may exert their influence on behavior. Only a few studies have examined correlations of brain activity with choice-irrelevant SVs, but crucially a precise relationship between these signals and the behavioral slowing of non-value-based choices has not yet been established. This is primarily due to the fact that automatic or task-irrelevant SV signals have been investigated with paradigms that involved no choice at all (Levy et al., 2011), forced actions (Plassmann et al., 2007), or hypothetical choices (Tusche et al., 2010), thereby precluding quantitative assessment of how choice-irrelevant SVs impact on task performance during value-unrelated decisions. Moreover, it is an open question whether any such automatic SV representations are functionally overlapping with or distinct from choice-dependent SV signals, as previous studies that have assessed automatic SV coding during value-unrelated tasks have either focused on only one region (Kim et al., 2007) or have pooled activity across several brain areas (Lebreton et al., 2009). Thus, it is unclear whether different regions of the brain's valuation circuitry contain functionally distinct SV representations that differentially relate to value-based choices or value-based attentional capture.

To address this issue, we developed a novel choice task in which human participants alternated between purchasing decisions (for which SVs are directly choice-relevant) or perceptual decisions (for which SVs are unrelated to the current choice). Both types of choices were taken based on identical visual stimuli and motor responses. This novel paradigm is ideally suited for various hypothesis tests that can identify brain regions where SV representations predominantly relate to value-based choices or to value-based attentional capture.

First, we hypothesize that if a brain region specifically represents choice-relevant SV, then value coding should be enhanced in the context of purchasing compared to perceptual choices. This prediction stems from the well-documented effect that directing attention toward a specific stimulus feature enhances the sensitivity of visual neurons selective for that feature, typically by sharpening the neuronal tuning curve (Knudsen, 2007; Martinez-Trujillo and Treue, 2004; Reynolds and Chelazzi, 2004; Spitzer et al., 1988). This mechanism is thought to strengthen the neuronal representation of task-relevant features relative to background activity, thereby improving the signal-to-noise ratio and increasing the reliability of the neural signal used to control behavior (Kastner et al., 1999; Martinez-Trujillo and Treue, 2004; Moran and Desimone, 1985; Reynolds et al., 2000). We thus hypothesize that a similar mechanism may boost neural SV representations when these become choice-relevant. Any region in the brain representing predominantly choice-relevant SVs should exhibit a significantly steeper slope of the regression of neural activity on increasing SVs during purchasing compared to perceptual choices.

Second, we expect that these enhancements of neural SV representations are a critical determinant of the choice outcome. In general, attention-related activity modulations in functionally specialized regions are thought to result in higher reliability of the choice-relevant signals, thereby decreasing trial-to-trial variability of behavior for any constant stimulus (Desimone and Duncan, 1995; Knudsen, 2007; Luck et al., 1997). Thus, we hypothesize that the strength of the increase in SV representations during purchasing choices compared to the perceptual task will correlate with higher SV consistency across choices. SV consistency in this context means that if an item A is assigned a higher value than monetary amount X on a first occasion, then item A is also assigned a value higher than X when evaluated at a later time point (Rangel et al., 2008). In addition, we expect based on previous

findings (Knutson et al., 2007) that regions implementing choice-relevant SV representations should also contain signals that predict the actual purchasing choice.

In contrast to these hypotheses about choice-relevant SV representations, we expect that brain activity in regions representing SVs automatically (i.e. even when these are choice-irrelevant) will show a constant relationship to SVs for both purchasing and perceptual choices. This is because such regions encode SVs of potential choice options without being affected by the current task, and therefore in a similar fashion for both types of decisions (Kim et al., 2007; Lebreton et al., 2009). However, the strength of this automatic SV-related activity should relate to the degree of value-driven attentional capture for perceptual choices. That is, we expect that the strength of neural activity in any region representing SVs in an automatic fashion should correlate with the reaction time slowing observed during perceptual choices. This effect is thought to reflect that these neural SV representations automatically capture attention and therefore systematically slow down the unrelated perceptual choice (Anderson et al., 2011; Awh et al., 2012).

We directly tested these hypotheses for all putative valuation regions of the human brain, using functional magnetic resonance imaging (fMRI) in a sample of 26 healthy volunteers who took purchasing or perceptual choices on identical visual stimuli. This allowed us to measure and compare the neural response profiles for SVs when these were choice-relevant (during purchasing choices) or unrelated to the present decision (for perceptual choices). Moreover, we could directly relate the strength of these two types of value representations to SV consistency and choice outcome for value-based choices, or to value-based attentional capture during perceptual choices.

RESULTS

Behavioral Results

Both types of decisions were based on the same visual stimuli (DVD movie covers, each presented only once per decision type **Figure 1A-B**) and were carefully matched for identical motor responses and reaction times (**Figure 1D-F**). Reaction times (RT) in both tasks did not significantly differ (t_{25} = -0.17, P = 0.86, paired t test, **Figure 1D-E**) but were strongly correlated across participants, indicating that both types of choices did not entail fundamentally different processing demands (r = 0.82 p < 0.001, **Figure 1F**). SV for each movie was quantified by willingness-to-pay ratings (Becker et al., 1964) (between 0-20 Swiss francs for 672 movies) - a standard method widely used in behavioral economics and neuroeconomics (Krajbich et al., 2010; Plassmann et al., 2007) – which were provided by each participant 1-3 days prior to fMRI.

During scanning, SVs were directly relevant for the purchasing decisions, which required the participants to choose whether or not to buy the depicted movie at an aurally presented price that varied around the predetermined SV. In contrast, SVs were irrelevant for the matched perceptual decisions, in which participants judged whether the numbers of faces (FV) present on the DVD cover matched an aurally presented number that varied around the actual FV (see **Experimental Procedures** for details). Importantly, SV and FV were uncorrelated in both tasks (t_{25} = -1.34, P = 0.19, **Figure 1C**), therefore allowing unbiased analyses of how SVs are neurally represented during both types of choices.

We confirmed that SV was indeed choice-relevant for purchasing decisions and choice-irrelevant for perceptual decisions using multiple logistic regression analyses of participants' behavioral responses. This showed that the difference between SV and the aurally presented price strongly affected accept/reject purchasing choices (t_{25}

= 9.24, $P = 1.5*10^{-9}$, **Figure 2A**, one-sample *t* test, see **Experimental Procedures**) but not perceptual choices (t_{25} = -1.62, P = 0.12, **Figure 2B**). Conversely, the absolute difference between FV and the aurally presented number strongly affected perceptual choices (t_{25} = -16.03, $P = 1.1*10^{-14}$, **Figure 2B**) but not purchasing choices (t_{25} = 1.37, P = 0.18, **Figure 2A**). These analyses thus confirm that participants indeed based their choices exclusively on SVs for value-based choices and on FVs for perceptual decisions.

To test whether our data also exhibit the predicted value-driven attentional capture effect (i.e., slowing of perceptual choices with increasing choice-irrelevant SV (Anderson et al., 2011), we regressed RTs of perceptual decisions on the trial-wise SV and FV (**Figure 2D**). Unsurprisingly, we found that RTs increased with an increasing number of faces participants had to match (FV; t_{25} = 14.35, $P = 1.4*10^{-13}$), but crucially, we also found a significant RT increase proportional to the choice-irrelevant SVs of the DVDs (t_{25} = 3.66, $P = 1.2*10^{-3}$). This confirms engagement of a value-driven attentional capture mechanism during perceptual choices. The speed of purchasing decisions was also affected by choice-relevant SV (t_{25} = 2.22, P = 0.036, **Figure 2C**) but not by the number of faces on the cover (t_{25} = 0.76, P = 0.45, **Figure 2C**), thereby further confirming that participants were only affected by SVs (and not FVs) when taking value-based choices.

Functional Imaging Results

The primary aim of the fMRI analyses was to compare how automatic and choice-dependent value representations are implemented in the human brain. To this end, we took great care to ensure that experimental stimulation (visual/auditory), RTs and motor responses were identical across both types of choices. This precise match in sensory and motor-related neural processing between both types of decisions was

reflected in the substantial overlap of blood oxygen level-dependent (BOLD) activity in audio-, visual-, and motor-associated regions common to both types of choices (conjunction analysis all $P < 0.05$, FWE-corrected, **Figure 3A**, see **Table S1**). Nevertheless, the differences in dependence on value-related or perceptual processing between purchasing and perceptual choices was already evident when comparing mean BOLD activity differences between both types of choices, averaging across all levels of SV and FV. Regions routinely associated with subjective valuation (such as the mPFC and PCC; see (Bartra et al., 2013; Clithero and Rangel, 2013), were significantly more activated during purchasing decisions than during perceptual decisions, whereas regions of the so-called dorsal attention network (i.e., inferior parietal sulcus (IPS), frontal eye fields (FEF)); see (Corbetta et al., 1991; Corbetta and Shulman, 2002)) as well as the lateral occipital complex (LOC) were significantly more activated during perceptual as compared to purchasing choices (all $P < 0.05$, FWE-corrected, **Figure 3B**, see **Table S2** & **S3**). These results confirm that despite their identical sensory and motor demands, the two types of decisions in our paradigm flexibly recruited regions that are functionally specialized for processing the information relevant for the current choice.

Two Distinct Types of Value Representations in the Brain

To distinguish choice-related versus automatic value computations in the human brain, we tested for neural activity that either represented SVs predominantly when these were task-relevant or that coded value irrespective of current behavioral goals. For this purpose, we regressed BOLD signals against the trial-wise SV of the DVDs during purchasing decisions - when the choice strongly depended on SV – and during perceptual decisions, in which SVs were irrelevant for the current choice. This analysis revealed that both types of SV representations are encoded in the brain, but

in clearly dissociated regions of the valuation system. On the one hand, BOLD signals in mPFC (**Figure 4A, C, E, G**) and bilateral VS (**Figure S1** and **Table S4**) significantly correlated with SVs during purchasing decisions but not during perceptual decisions, suggesting that both these regions mainly represent values when these are choice-relevant. Importantly, a direct contrast between purchasing and perceptual decisions confirmed that activity in both mPFC and VS showed significantly stronger correlations with SVs during purchasing decisions compared to perceptual decisions (**Figure 4C, E, G** and **Figure S1B, C, D**). We also note that this BOLD signal enhancement during purchasing choices was indeed related to the SVs of the DVDs and did not reflect the varying levels of prices presented alongside the items (see supplemental results section for the relevant control analyses).

In contrast to mPFC and VS, BOLD signals in the PCC (**Figure 4B, D, F, H)** showed similar positive correlations with both choice-relevant SV during purchasing decisions and choice-irrelevant SV during perceptual decisions. Note that correlations with SV during perceptual choices were also found for other areas such as bilateral dorsolateral prefrontal cortex (dlPFC) and bilateral parietal lobule (**Figure S2** & **Table S5**). This may possibly index a function of these areas in the filtering of distracting stimuli during perceptual choice (Friedman-Hill et al., 2003; Lennert and Martinez-Trujillo, 2011). However, the PCC was the only region that represented SVs both when these were relevant and irrelevant for the current decision **(Figure 4D**, **F, H**), thereby fulfilling our requirements for an area that contains truly automatic, choice-independent value representations.

Our data therefore demonstrate a functional dissociation between brain regions consistently linked to value processing (Bartra et al., 2013; Clithero and Rangel, 2013). While the PCC represents SV in an automatic fashion that is invariant to

current behavioral aims, the mPFC and VS represent subjective value predominantly when it is relevant for the current choice.

Medial prefrontal cortex activity relates to value-based choice consistency

We next tested whether the strength of the choice-dependent SV representations related to the behavioral consistency of value-based choices. Consistency here refers to how well the participants' choices in the scanner agreed with their BDM-auction rating for each DVD provided 1-3 days prior to scanning (Becker et al., 1964; Krajbich et al., 2010; Plassmann et al., 2007). That is, a choice is SV-consistent if participants purchase a DVD when its price is less than or equal to the value they stated previously, or if they decline to purchase a DVD when its price is above their previously stated value. A relation between SV conistency and neural SV representations was expected because stronger neural choice-relevant value responses result in an enhanced signal-to-noise ratio and thus more reliable behavioral readout of the values across both testing occasions. We tested for such a consistency effect with a linear mixed-effects regression of the proportion of consistent choices on the average strength of the neural choice-relevant value responses (this analysis was conducted across value quintiles, see Experimental Procedures for details). Note that the data submitted to these analyses were extracted from regions-of-interest that were independently defined by the leave-one-subject-out (LOSO)-procedure to avoid circularity (Esterman et al., 2010; Kriegeskorte et al., 2009; Poldrack and Mumford, 2009); see Experimental Procedures for details).

Only the mPFC showed a relationship between the magnitude of BOLD response and choice-consistency (X^2 = 4.85, p = 0.027, likelihood ratio test) while no such relationship was found for PCC (X^2 = 0.23, p = 0.629) and only a trend emerged for

VS (X^2 = 2.43, p = 0.12), (**Figure 5A** & **Table S8**). Importantly, the strength of value-related BOLD activity in the mPFC was more strongly related to choice consistency than the corresponding PCC activity (X^2 = 6.49, p = 0.01, likelihood ratio test; **Table S8**), suggesting that the value signals in mPFC are more relevant for purchasing behavior than SV signals from task-invariant PCC. The data regarding stronger involvement of the VS as compared to PCC are inconclusive, as they revealed only an effect at trend-level (X^2 = 2.38, p = 0.13).

We also tested whether SV consistency was specifically related to the strength of the choice-related value enhancement process, rather than to neuronal value coding per se. That value-based consistency is not driven by a mere correlation with SV per se is already evident from the finding that the choice-relevant value responses in the PCC did not relate to the proportion of SV-consistent choices. If the choice-related enhancement of value responses indeed increases the fidelity of value coding, then SV consistency should relate to the strength of the difference between the choice-relevant and choice-irrelevant value response profile. We again tested this hypothesis with linear mixed-effects analyses (see **Experimental Procedures** for details). This revealed a significant relationship only in the mPFC (X^2 = 4.12, p = 0.042, likelihood ratio test) but not in PCC (X^2 = 0.36, p = 0.55) or VS (X^2 = 0.01, p = 0.94). Crucially, the value signal enhancement in mPFC accounted for value-based consistency significantly better than the corresponding enhancement in the PCC (X^2 = 3.78, p = 0.05) or the VS (X^2 = 4.95, p = 0.026). Thus, these findings suggest that the enhancement of value representations in the mPFC during purchasing decisions specifically increases the stability of these representations and thereby leads to more consistent value-based choices.

Relating neural signals to purchasing choices

Previous studies (Knutson et al., 2007; Padoa-Schioppa, 2013; Strait et al., 2014) have shown that valuation regions contain signals that can be used to predict choice outcomes. We therefore expected that regions containing choice-relevant SV signals should - in addition to supporting consistent valuation of items across decision contexts - also provide information about whether or not a DVD will be purchased in our task. We tested this hypothesis with analyses of how purchasing decisions on any given trial can be predicted by BOLD activity in the mPFC, VS and PCC. To this end, we performed a receiver operating characteristic (ROC) analysis (Green and Swets, 1966) that quantifies the reliability with which the single-trial amplitude of the BOLD signal - at various timepoints following stimulus onset - predicts the purchasing choice on that trial (see **Experimental Procedures** for details). Consistent with previous reports (Knutson et al., 2007), we find that BOLD signals in the mPFC within 4 to 8 seconds post-stimulus significantly predict purchases, while the corresponding signals extracted from PCC do not (**Figure 5B**). The response timing of this relationship is similar to the peak delay and temporal spread of the hemodynamic response, suggesting that the mPFC activity that predicts purchases is associated with the decision period lasting from 0-1.7 seconds after trial onset. Importantly, within this time period between 4 to 8 seconds after stimulus onset, the mPFC predicts purchases significantly better than the PCC (paired t test, $p < 0.05$, two-tailed, **Figure 5B**). Note that we do not find purchasing-predictive activity in the VS (see **supplemental Figure S3**), again in line with previous reports examining similar fixed-price purchasing decisions as employed here (Knutson et al., 2007).

Posterior Cingulate Cortex Activity Relates to Value-Driven Attentional Capture

The BOLD signal response profile observed in the PCC suggests that this region is involved in automatic value coding, as it exhibits context-invariant value representations that are similar during purchasing and perceptual decisions. We therefore examined whether the choice-irrelevant value representations during perceptual decisions reflect automatic SV computations that may facilitate attentional orienting to valuable items outside the current focus of attention. To this end, we tested whether the strength of choice-irrelevant SV representations during perceptual decisions related to the degree of value-based attentional capture, i.e., the behaviorally observed reaction time slowing of perceptual choices with increasing SVs (Anderson et al., 2011). We tested this hypothesis for all three regions that were found to represent choice-irrelevant SVs (PCC, dlPFC and parietal Lobule) using linear mixed-effects analyses (again, these analyses were performed on data binned into SV quintiles, see **Experimental Procedures**). Only signals in the PCC showed the predicted significant relationship between perceptual reaction times and choice-irrelevant SV response strength (X^2 = 9.83, p < 0.002, likelihood ratio test) (**Table S9**). Additionally, PCC value signals accounted for this effect more strongly than corresponding signals in the dlPFC (X^2 = 10.27, p = 0.001) and parietal lobule (X^2 = 11.45, p = $7*10^{-3}$) (**Table S9**). For completeness, we also compared the strength of this relationship between the PCC and the mPFC and VS, even though the latter two regions did not actually contain any significant SV representations during perceptual choices (see above). This confirmed that choice-irrelevant SV signals from PCC explained the degree of value-based attentional capture significantly better than the corresponding activity in mPFC (X^2 = 5.74, p = 0.016) and VS (X^2 = 9.08, p = 0.003). These results demonstrate that the strength of automatic neural SV representations in the PCC directly relates to the degree to which choice-irrelevant SVs slow down

perceptual performance, consistent with the idea that these PCC signals are involved in value-based attentional capture during perceptual choices.

DISCUSSION

Our study identified two distinct types of value coding mechanisms in the human brain, by comparing value representations and their relation to behavior during two choice situations in which SVs were either relevant or unrelated to the present choice. Our results revealed a clear functional dissociation between different regions of the human brain's valuation circuitry. SV representations in the mPFC were enhanced when SVs became choice-relevant and the strength of this enhancement related to the consistency and outcomes of choices. In contrast, SV representations in the PCC were invariant across contexts and related to value-driven attentional capture when SVs were irrelevant for the choice.

The sharpening of SV response profiles in mPFC and VS may reflect behaviorally relevant increases in signal-to-noise ratio similar to the sharpening of neuronal tuning curves associated with attention that lead to enhanced perceptual sensitivity (Knudsen, 2007; Martinez-Trujillo and Treue, 2004; Reynolds and Chelazzi, 2004; Spitzer et al., 1988). This sharpening process may provide a mechanistic explanation for recent findings that attention can change value-based choices and related neural activity. For instance, fMRI activity in the mPFC can be increased when participants direct attention to the affective value (vs perceptual intensity) of a stimulus (Rolls and Grabenhorst, 2008) (cf. **Figure 3B)**. Moreover, visual fixation of one item from a choice set is associated with a higher probability of choosing that item over the others (Krajbich et al., 2010) and can determine whether its SV impacts negatively or positively on neural activity in the mPFC and VS (Lim et al., 2011). Furthermore, computational models that include an attentional modulation term of the relative

model inputs account better for several aspects of value-based choice behavior than models that do not incorporate attention or fixation patterns (Krajbich et al., 2012; Towal et al., 2013). Finally, non-human primates with mPFC lesions exhibit deficits in focusing on the most relevant comparison in a three-option task (Noonan et al., 2010) and addition of a third choice option changes mPFC value signals and choices between two constant stimuli (Chau et al., 2014).

While all these previous findings suggest that attention-related mechanisms can influence value-based choices and SV-related BOLD signals, our study clearly demonstrates that attention to a single item's SV leads to an enhancement of its value representation in the mPFC, and that this signal enhancement directly relates to the consistency and outcome of purchasing choices. These effects therefore provide a value-based analogue to findings from the perceptual literature on the relation between behavioral effects of covert attention and corresponding neural modulations observed in visual cortex (Reynolds and Heeger, 2009). These neural effects of attention are thought to improve the fidelity of the neural signal and thereby the reliability of the choice-relevant information (Desimone and Duncan, 1995; Kastner et al., 1999; Knudsen, 2007; Luck et al., 1997; Martinez-Trujillo and Treue, 2004; Moran and Desimone, 1985; Reynolds et al., 2000). Please note in this context that the observed task-related modulations of SV coding were clearly distinct from corresponding effects on FV representations relevant for the perceptual choices: Contrasting choice-relevant and choice-irrelevant FV effects for perceptual choices (**supplemental Table S6 & S7**) revealed the precise activation pattern in parietal cortex and frontal eye fields that one would predict from studies that contrasted active attention conditions to passive fixation (**Figure S4**)(Culham et al., 2001; Kanwisher and Wojciulik, 2000).

Our findings also have bearings on previous studies investigating choice-relevant and choice-irrelevant SV representations with seemingly contradictory results (Lebreton et al., 2009; Plassmann et al., 2007). Lebreton et al. described the ventromedial PFC as part of a multi-region brain valuation system that shows automatic choice-irrelevant SV coding, whereas Plassmann et al. find this region to correlate stronger with SV in free (SV-relevant) than in forced (SV-irrelevant) value-based choices. These conflicting conclusions may reflect differences in analysis methodology. While Plassmann et al. performed a whole-brain voxel-wise analysis as employed by the present work, Lebreton et al. pooled activity across several regions (including mPFC, VS, and PCC), therefore precluding the possibility of region-specific inference. It is possible that the features of the automatic SV representations reported by Lebreton et al. are mainly driven by the PCC. Another possible explanation for the divergent findings relates to the nature of the behavioral paradigms. The non-value-related tasks used by Plassmann et al. and ourselves required an evaluation/action that could be objectively correct or wrong and was fully unrelated to the item's value. In contrast, the SV-irrelevant task used by Lebreton and colleagues required the participants to subjectively evaluate the age of the stimulus in unspeeded choices, which may have triggered concomitant assessment of the items' subjective value (i.e., the age of a painting/house/person usually has implications for its value to an observer). Further studies may be required to distinguish between these explanations and fully resolve these inconsistencies.

We found that the strength of value-related activity in the PCC correlated with the degree by which reaction times were slowed for perceptual decisions. These results suggest a crucial role for the PCC in automatic value coding and value-driven attentional capture. Our findings may thus have important implications for a large body of data on shifts of attention as studied with electroencephalography (EEG).

The crucial scalp component associated with shifts of attention (N2pc)(Eimer, 1996) has consistently been associated to parietal-occipital scalp sites (Luck and Hillyard, 1994; Woodman and Luck, 1999), including cases in which the targets were associated with higher compared to lower rewards (Kiss et al., 2009). The precise neuroanatomical source for these effects, however, is difficult to locate with EEG. Our data suggest that the PCC may be a likely origin for the parietal-occipital N2pc component, at least in situations where previously unattended values of visual objects capture attention.

The automatic nature of SV representations in PCC may constitute an important evolutionary advantage, as it could ensure that subjective values of external environmental features are continuously encoded with minimal use of attentional resources, in order to trigger behavioral engagement with alternative courses of action whenever this is beneficial. This proposed function is in line with recent findings that in volatile environments, macaque PCC neurons encode dynamic signals that are used for the decision to explore alternative actions in the future (Hayden et al., 2008). Moreover, our results also appear consistent with findings that macaque PCC neurons are involved in change detection and policy control during reward-guided behavior (Pearson et al., 2011), by contributing to the automatic detection of a superior option (based on prior experience or reward history) and the subsequent actions taken to either exploit or explore alternative options (Pearson et al., 2009). All these proposals support the view that the PCC may play a crucial role in optimizing reward-based behavioral control by evaluating alternative courses of actions (Heilbronner and Platt, 2013), and the neural computations necessary for this function may arrest or at least slow down current behavior as observed in value-based attentional capture.

We found two additional regions, bilateral dlPFC and bilateral parietal lobule, that coded irrelevant SV during perceptual choices. Both regions are part of a broader brain network involved in the control of cognitive functions such as working-memory and spatial attention (Constantinidis and Procyk, 2004; Corbetta and Shulman, 2002; Todd and Marois, 2004). The two areas are tightly interconnected and share many functional properties, but importantly have been assigned a crucial role in maintaining a stimulus in working memory and filtering distracting stimuli (Katsuki and Constantinidis, 2012). Thus, it is possible that these two areas worked to counteract the automatic SV effects triggered by the PCC to prevent the increasing interference of stimulus value with the perceptual task demands. This interpretation is consistent with the finding that the two regions only coded SVs during perceptual choices, but not when the SVs became choice-relevant during the purchasing decisions.

Taken together, our results demonstrate a fundamental functional dissociation between different brain regions whose contributions to reward representation and value-based choice have, thus far, been largely indistinguishable (Bartra et al., 2013; Clithero and Rangel, 2013). In the mPFC, SV representations reflect a choice-dependent value coding mechanism that is enhanced when SV becomes relevant for the decision at hand. These value-related neural responses in the mPFC carry information related to choice consistency and can be used to predict purchases. In the PCC, by contrast, SV representations are invariant across situations where SV is relevant or irrelevant for current behavior, and the strength of this automatic SV representation relates to value-driven attentional capture. The PCC may therefore play a crucial role in facilitating shifts of attention towards valuable items or actions outside the current focus of attention. The functional dissociation observed here suggests that disruptions of each of these two mechanisms will have distinct impacts on behavior. Direct comparisons of choice-dependent and automatic value coding in

the brain may therefore help in diagnosing and potentially treating pathological disturbances of value-based behavioral control in the context of brain disorders such as addiction (Berridge, 2012; Davis, 2010; Field and Cox, 2008), attention deficit/hyperactivity disorder (Castellanos and Proal, 2012; Davis, 2010) and autism (Sasson et al., 2011; Sasson et al., 2008).

EXPERIMENTAL PROCEDURES

Participants.

Twenty-six subjects (20-28 years old; 13 males) provided informed consent as approved by the Research Ethics Committee of the Canton of Zurich. All subjects had normal or corrected-to-normal vision, were in good health and reported no current use of medication as measured with standard surveys.

Rating session.

One to three days prior to functional imaging, subjects were given an allowance of CHF 20 and rated their willingness to pay (between 0-20 CHF) for each of 672 movies in a Becker-DeGroot-Marshak auction (BDM) (Becker et al., 1964). The optimal strategy in this setting was to truthfully indicate the subjective value (SV) of each movie (Krajbich et al., 2010; Plassmann et al., 2007). During each trial of the auction, the movie cover and title were presented for 1 sec; the title remained on screen until the subject entered their SV via computer keyboard. Entered values were displayed on the screen and could be changed until the subject finalized their choice by pressing the enter key. Subjects were allowed to rate at their own speed but every 100 trials short breaks were suggested. The rating lasted between 40-60 minutes.

fMRI Task.

During the event-related fMRI sessions (**Figure 1A-B**), subjects took either purchasing or perceptual choices in randomly alternating blocks, thereby changing between choice setting in which SVs of the movie were choice-relevant (purchasing choices) or choice-irrelevant (perceptual choices). Both blocks were cued visually and aurally. For both types of decisions, participants viewed the same DVD covers, heard numbers via headphones, and indicated their choices via the same two response buttons. For purchasing decisions, subjects indicated whether the number represented an amount they were willing to pay for that movie (Plassmann et al., 2007). SV was therefore choice-relevant, because subjects had to evaluate whether their SV for the DVD was high enough to pay the stated price. For these trials, participants were endowed with an allowance of 20 CHF to spend, and one trial was randomly selected and the decision on that trial was implemented after the experiment. During perceptual decisions, subjects indicated whether the presented number matched the number of faces on the cover. The SV of the DVD was therefore choice-irrelevant. This allowed us to assess and compare its representation between two contexts that differed in SV relevance but that were matched in sensory input, motor response, and reaction time (**Figure 1D-F**).

In order to encourage active engagement and attentional focus on the choice-relevant stimulus dimension (SV or number of faces [FV]), the covers were slightly phase-randomized as in (Rieger et al., 2013), ensuring a perceptual accuracy level between 75% and 95% correct FV detections as determined from pilot data on 21 subjects. Importantly, the identical covers were presented for purchasing and perceptual choice trials, thereby keeping sensory stimulation constant. For each purchasing choice, the auditory offer number was chosen from a uniform discrete distribution bracketing the SV (possible difference to SV: -4, -2, 0, +2, or +4 CHF).

For perceptual choices, the number varied uniformly around the true number of faces (by -2, -1, 0, +1, or +2). We defined purchasing decisions as value-consistent if participants accepted auditory offers equal or below the SV or rejected offers that were higher than the SV (all other choices were defined as value-inconsistent). The subject-specific SV values for the DVDs were determined prior to the choice task using the BDM auction procedure. Perceptual choices were defined as correct if participants accepted auditory offer numbers that matched the actual face number, whereas all other choices were incorrect.

To ensure full independence of the two types of choices, DVD covers were carefully selected for each participant based on the initial rating session. Movies that received a BDM bid of zero were excluded. For the final set of movies used in the experiment, the number of faces present on the cover (1-8) was not correlated with the subjective value (1-20 CHF) of the movies (linear regression: mean standardized estimate = -0.234, t_{25} = -1.3398, P = 0.1924, one-sample t test, **Figure 1C**). We further controlled for possible confounding effects of adaptation by presenting each DVD-cover exactly once as a purchasing choice and once as a perceptual decision (with randomly determined order). Potential attention and saliency confounds between the two tasks were counteracted by ensuring that the SV and face-number frequency distributions followed the same shape. This was ascertained by fitting gamma probability-density functions using maximum likelihood estimation to the shapes of the SV and face-number distributions for each subject, which revealed no significant difference (t_{25} = 1.59, P = 0.11, paired t test on single subject shape parameter). Additionally, it is worth noting that the SV range used here (1-20 CHF) was based on naturally occurring market values, therefore precluding the necessity for any prior associative learning that may have differentially taxed memory capacity between the two types of decisions (Anderson et al., 2011).

Behavioral analysis.

To confirm that participants followed the task instructions and chose based on the difference between SVs and the price (for purchasing decisions) or the match between the perceptual criterion and the number of faces on the cover (for perceptual decisions), we regressed accept/reject choices in both tasks against (SV-Offer) and (|FV-Offer|) using within-subject multiple logistic regression with the formula:

$$P_{accept} = \frac{1}{1 + \exp\left(-(\beta_0 + \beta_1(\mathrm{SV} - \mathrm{Offer}) + \beta_2(|\mathrm{FV} - \mathrm{Offer}|)\right)}.$$

To test for attentional capture by choice-irrelevant SV during perceptual choices, we performed a within-subject multiple linear regression of reaction times on each DVD's SV and FV (SV should result in a slowing of perceptual choices if it captures attention despite not being choice-relevant) with the formula:

$$RT = \beta_0 + \beta_1 SV + \beta_2 FV .$$

The resulting individual regression parameter estimates were standardized and their significant deviance from zero was tested using a two-sided t-test.

fMRI data-acquisition and pre-processing.

Subjects performed ten choice-task-sessions (each containing 30 purchasing and 30 perceptual choices) and one resting-state-session that lasted 6.5 minutes each. During each session, we acquired 147 T2*-weighted whole-brain echo planar images using a Philips Achieva 3 T whole-body scanner (Philips Medical Systems, Best, The

Netherlands) equipped with an 8-channel Philips sensitivity-encoded (SENSE) head coil. Imaging parameters were: 2600 ms repetition time (TR); 37 slices (transversal, ascending acquisition); 2.6 mm slice thickness; 2.5 mm x 2.5 mm in-plane resolution; 0.65 mm gap; 90° flip angle. To measure at fully equilibrated magnetic field, five dummy image excitations were performed and discarded before functional image acquisition started. To enhance BOLD-contrast sensitivity throughout the brain, we used a dual-echo-sequence (TE: 17 ms and 44 ms) in combination with a weighted voxelwise summation technique (Posse et al., 1999; Schmiedeskamp et al., 2010) that generates a single functional whole-brain image with optimal sensitivity for each TR. For this procedure, the signal-to-noise ratio is first computed for each echo image voxel in the resting-state scan. These SNR measures are then used to weight each voxel in the two echo images acquired per TR of the choice-task sessions according to the formula

$$X = \frac{X_{E1} \cdot SNR_{E1} + X_{E2} \cdot SNR_{E2}}{SNR_{E1} + SNR_{E2}},$$

where *X* is the resulting image for a given TR, and are the images acquired at that TR for the first echo and second echo, respectively, and and are the signal-to-noise images (generated as voxel-wise mean divided by the voxel-wise standard deviation) for the resting-state timeseries acquired for the first echo and second echo, respectively. A high-resolution T1-weighted whole brain structural image (1 x 1 x 1 mm) was also acquired for each subject.

Peripheral measures.

We controlled for the effects of eye movements, blinks, pupil size, breathing and heart rate on fMRI activity by controlling for measures of these physiological processes in our statistical analyses. During scanning, eye movements were sampled at 500Hz using an MR-compatible infrared EyeLink II CL v4.51 eye-tracker system (SR Research Ltd.). Saccades were defined as eye movements larger than 0.5 degrees visual angle. Blinks were defined as periods of signal loss lasting longer than 80 ms and shorter than 2000 ms; these epochs were removed from the pupil data by linear interpolation. Measures of cardiac and respiratory signals were obtained using four electrodes and a pressure belt placed around the umbilical region, respectively. Correction for this physiological noise was performed via RETROICOR (Glover et al., 2000) using Fourier expansions of different order for the estimated phases of cardiac pulsation (3rd order), respiration (4th order) and cardio-respiratory interactions (1st order) (Harvey et al., 2008). The corresponding confound regressors were created using a custom in-house Matlab implementation (Hutton et al., 2011; Kasper et al., 2009).

fMRI data-analysis.

Image preprocessing and analysis were conducted using SPM8 (Wellcome Trust Centre for Neuroimaging). Images were slice-time corrected (to the middle slice acquisition time) and realigned (accounting for subjects head motion). Each subjects' T1-weighted structural image was co-registered with the mean functional image and normalized to the standard T1 MNI template using the new-segment-procedure provided by SPM8 (Ashburner and Friston, 2005). The functional images were then normalized to the standard MNI template using the same transformation, spatially

resampled to 3 mm isotropic voxels, and smoothed using a Gaussian kernel (FWHM, 8mm).

We estimated five general linear models. The main GLM was designed to identify and contrast correlations of BOLD signals with choice-relevant SV and choice-irrelevant SV during purchasing and perceptual choices, respectively. It therefore contained the following regressors: First, an indicator function for purchasing choices onsets with three parametric modulators (1^{st}: choice-irrelevant FV, 2^{nd}: choice-relevant SV, 3^{rd}: price, i.e., the auditory offer number). Second, an indicator function for perceptual choices onsets with three parametric modulators (1^{st}: choice-irrelevant SV, 2^{nd}: choice-relevant FV, 3^{rd}: auditory offer number). Trial duration length in our GLMs was set to the reaction time on that trial. Each of the regressors was convolved with a canonical hemodynamic response function and regressed against the blood oxygen level-dependent (BOLD) signal in each voxel.

The second and third GLMs were estimated to extract parameter estimates from regions of interest that could be used to visualize choice-relevant and choice-irrelevant SV representations (**Figure 4E-H & Figure S1C,D**) and to relate brain activity to choice consistency and value-driven attentional capture (see below and supplemental **Table S8** and **Table S9**). We created five levels of SVs and FVs by partitioning each participant's trials into quintiles (20-percent bins) based on their individual SV and FV distributions. The onsets of the trials contained in each SV or FV quintile then entered as indicator functions into the two additional GLMs. The second GLM thus contained five indicator functions for the onsets of purchasing choices corresponding to the choice-relevant SV quintiles and five indicator functions for onsets of perceptual choices contained in the choice-relevant FV quintiles. The third GLM was identical to the second GLM, but now trials were sorted into quintiles

according to the corresponding choice-irrelevant FVs (purchasing choices) and SVs (perceptual choices).

The purpose of a fourth GLM was to test whether regional differences in SV coding observed with the main GLM would differentially depend on whether the aurally presented price was below or above the SV. GLM 4 was identical to the main GLM (see above) but crucially the trial indicator functions were separately assigned to trials where the price was below or above the SV. We then compared the individual whole brain maps for the contrast [choice-relevant SV > 0] and [choice-relevant SV-choice-irrelevant SV] using paired t-tests. These analyses were performed both at the whole-brain level and for the relevant regions-of-interest (ROI), which were defined independently using the (LOSO)-procedure to avoid circularity (see below).

The fifth GLM assessed whether the price-value difference explains any additional variance beyond that of SV in the BOLD signal during purchasing choices. GLM 5 was identical to the main GLM except that the parametric modulator for price was substituted by the price-value difference. The group effect of price-value difference was then tested for significance using second-level statistics (see below).

All GLMs modeled MR image auto-correlations with a first-order autoregressive model and also included the following regressors of no interest: Two indicator functions for purchasing and perceptual block cues, 6 motion parameters (obtained during the realignment procedure), 18 physiological parameters (accounting for cardiac and respiratory fluctuations as well as their interaction, see above), and indicator functions for blinks, saccades and pupil activity. The last two regressors additionally contained a parametric modulation with saccade size and pupil size, respectively.

First-level summary statistics were obtained by calculating the single-subject voxel-wise contrasts of interest for the SV and FV parametric modulators, both when

choice-relevant and choice-irrelevant, as well as their respective interactions. Second-level random effects group contrast maps were then tested for significance by one-sample *t* tests on these single-subject contrasts (except for conjunctions, which were tested in a one-way ANOVA). Statistical inference was performed at the cluster level, using a whole-brain FWE-corrected statistical threshold of $P < 0.05$ (based on a cluster-forming voxel cut-off set to $P < 0.001$). For the hypothesis-guided ROI analysis of the ventral striatum (VS), we corrected for multiple comparisons using a small-volume correction (SVC, $P < 0.05$) within the bilateral nucleus accumbens volume mask provided by the FSL-Harvard-Oxford-atlas (http://neuro.debian.net/pkgs/fsl-harvard-oxford-atlases.html).

Relating neural activity to behavior.

All our analyses relating neural to behavioral measures were performed on data extracted using the leave-one-subject-out (LOSO)-procedure (Esterman et al., 2010), in order to prevent circularity and to ensure unbiased data extraction (Kriegeskorte et al., 2009; Poldrack and Mumford, 2009). The LOSO-procedure first uses the data from n-1 subjects to determine the peak activation for a contrast in a given region, and then extracts BOLD signals from a sphere (here of 5 mm radius) around this peak for the independent subject that was not included in n-1 analysis to determine the ROI. An n-fold replication of this procedure thus ensures that for each subject, the peak coordinates have been determined from an independent sample of participants, thus avoiding double-dipping and selection biases (Kriegeskorte et al., 2009; Poldrack and Mumford, 2009).

In order to relate neural activity to value-based choice consistency, five levels of SVs were created by partitioning each participant's trials into quintiles, identical to the fMRI trial parcellation employed to generate GLM 2 and 3. We then computed the

proportion SV-consistent purchasing choices for each of these SV quintiles. Value-based choices were defined as consistent if a DVD with price ≤ SV was purchased or if a DVD with price > SV was not purchased. The fMRI data for these analyses from mPFC and PCC were extracted from ROIs defined with the LOSO-approach on the peak of the choice-relevant SV contrast (threshold of p = 0.0005 uncorrected), whereas the search space for the VS was confined to the nucleus accumbens volume mask provided by the FSL-Harvard-Oxford-atlas (**Figure S1A-B**).

To test the relationship between these extracted BOLD response profiles and behavior, we performed linear mixed-effects analyses to regress each participant's average purchasing choice consistency for each quintile on the extracted BOLD responses. In these analyses, BOLD responses were treated as fixed effects and we included intercepts for each participant as random effects. We determined a significant effect of activity in a specific region on behavior by means of a likelihood ratio test of the full model including activity from the region against the null model containing only the intercepts. Additionally, we tested for significant differences in explanatory power between regions by using likelihood ratio tests between full models containing two regions and reduced models with only one region. For instance, to compare the contribution of the mPFC to explaining accuracy beyond what can be explained by PCC signals, we compared the full model containing fixed effects for mPFC and PCC signals against the reduced model containing only PCC (**Table S8** & **Figure 5A**).

To test whether regions that code choice-irrelevant SV are involved in value-driven attentional capture, we used the identical linear mixed-effects analyses procedure as above, except that we now regressed reaction times during perceptual choices for each SV quintile on the corresponding SV BOLD responses during perceptual decisions. Individual BOLD response profiles were extracted from spheres (5 mm

radius) centered on peaks of the choice-irrelevant SV response, independently determined using the LOSO-procedure on the choice-irrelevant SV contrast (threshold of p = 0.0005 uncorrected) for PCC, bilateral dlPFC and bilateral parietal lobule (**Table S9** & **Figure 5C**).

In order to test whether trial-wise signals in the mPFC, VS and PCC also differ in their capability of predicting actual purchases, we extracted BOLD time series for each subject, run and ROI using LOSO as above (restricted to the choice-relevant SV contrast) and transformed them to percent signal change. To increase precision with respect to trial onset, the average time course for each region was interpolated to 100 ms intervals using a cubic spline. We quantified the reliability with which the single-trial amplitude of the BOLD signal predicted actual purchasing choices (purchasing versus not purchasing) using a receiver operating characteristic (ROC) analysis (Green and Swets, 1966), conducted at each 100 ms time point within the period of 1 second before and 13 seconds after the onset of a trial (**Figure 5B**). The area under the ROC (AUC) provides a measure of the separability of two conditions and can be used to test the statistical significance of the purchasing/not purchasing prediction from the BOLD data. AUC is widely employed for quantification of categorical predictions, for instance in single cell- (Reddy et al., 2006), EEG- (O'Connell et al., 2012) or fMRI-data (Skudlarski et al., 1999; Sorenson and Wang, 1996).

To estimate and compare the predictive power of BOLD signals in different ROIs for purchases, we estimated the z-statistic for each ROI, subject and time point. To this end, we first generated the null distribution of the area under the ROC curve for chance performance AUC_{chance} via 1,000 iterations of randomly shuffled trial labels while conserving the individual proportions of purchase/not purchase decisions. These computations were implemented independently for each time point *t*. For each

ROI and subject, the individual z-statistic Z_t was then computed at each time point *t* using the following formula:

$$Z_t = \frac{AUC_t - \mu_{AUC_{t\,chance}}}{\sigma_{AUC_{t\,chance}}},$$

Where $\mu_{AUC_{t\,chance}}$ represents the mean AUC of the 1,000 randomizations and $\sigma_{AUC_{t\,chance}}$ represents the standard deviation of the 1,000 randomizations. For each region, the average across subjects at each time point *t* yielded the group z-statistic at that time point. This index yields above-chance purchase predictability when the group z-statistic exceeds the critical value of 1.64, corresponding to a significance level of $p < 0.05$ one-tailed (please note that identical results are observed using the corresponding two-tailed significance threshold, $z > 1.96$). Group z-statistic comparisons between ROIs were conducted at each time point *t* using a paired t-test. This analysis allowed us to statistically examine whether we can predict a purchasing decision on a single trial basis.

AUTHOR CONTRIBUTION

M.G. and C.C.R. conceived the study.

M.G., T.A.H and C.C.R. designed the study.

M.G. performed experiments and analyzed data with conceptual input from R.P., T.A.H and C.C.R.

M.G., T.A.H and C.C.R. wrote the manuscript.

ACKNOWLEDGEMENT

We thank Karl Treiber for scanning assistance, Adrian Etter for support with the eye-tracking setup and Lars Kasper for providing software for the analysis of the peripheral physiological data. This work was supported by grants of the SNSF (105314_152891, CRSII3_141965 and 51NF40_144609) and the SNSF NCCR Affective Sciences to C.C.R. All authors gratefully acknowledge support by the Zurich Center for Neurosciences (ZNZ).

FIGURE LEGENDS

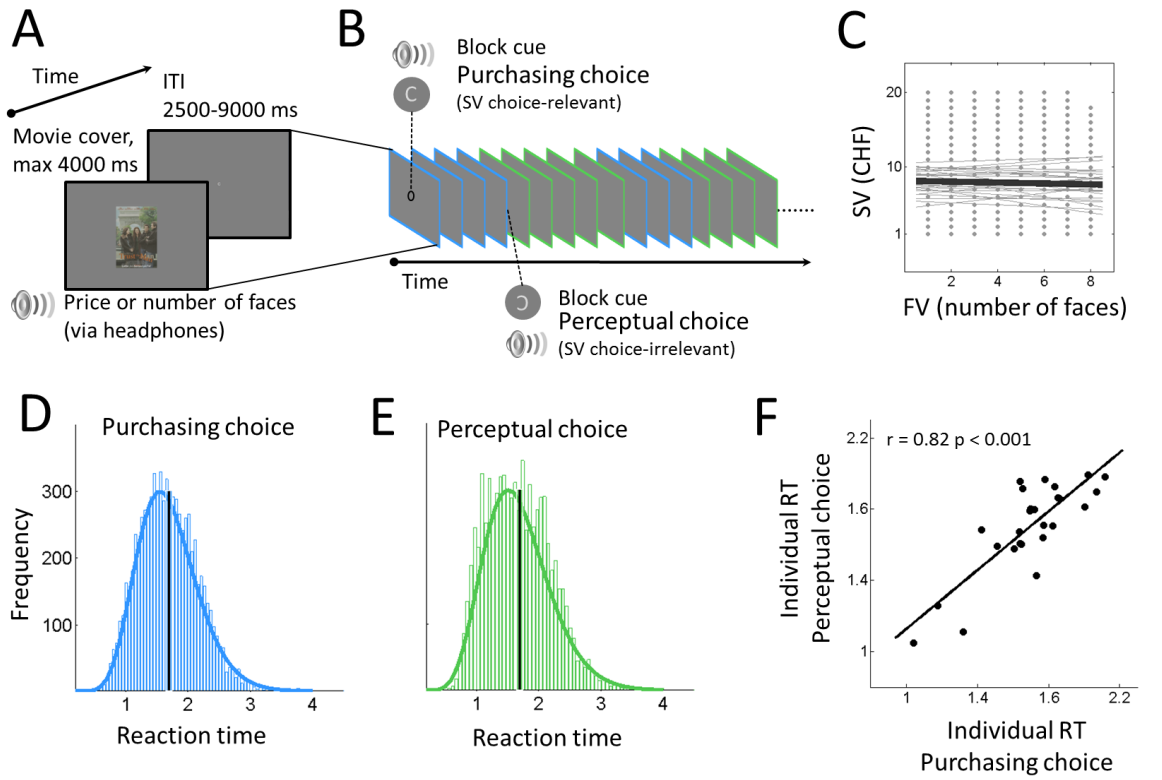

Figure 1. Experimental task and reaction time results.

(A) In the scanner, participants performed two types of choices on identical DVD-cover-stimuli (see also **Experimental Procedures** for details). For value-based choices (SV choice-relevant), participants indicated their willingness to pay a specified price for that movie under real purchasing conditions. For perceptual choices (SV choice-irrelevant), participants indicated whether the aurally presented number of faces matched the number of faces on the cover.

(B) Purchasing and perceptual choices were presented in randomly alternating mini-blocks of 3-5 trials each. The choice type was indicated prior to each block via an auditory cue. During each block, the choice type was furthermore indicated by a central visual marker (C for purchasing decisions and rotated C for perceptual decisions). Each movie-cover was presented only once for purchasing and

perceptual choices, respectively, in a randomized order to counteract possible novelty or memory effects.

(C) SV and FV were uncorrelated in both tasks (mean β = -0.234, linear regression, t_{25} = -1.3398, P = 0.1924, one-sample t test). Grey lines represent single subject regressions of FV on SV. Thick black line represents this regression across subjects. Grey dots indicate SV/FV combinations that occurred at least once during the experiment.

(D-E) Reaction time distributions for purchasing choices (SV choice-relevant) and for perceptual decisions (SV choice-irrelevant). Bars represent observed counts and smooth lines represent gamma probability density functions fitted to the underlying distributions using maximum-likelihood estimation. Vertical black lines represent the reaction time means, which were not significantly different (purchasing decisions = 1.694 sec, perceptual decisions = 1.7 sec; t_{25} = -0.17, P = 0.86, paired t test).

(F) Individual mean RTs were strongly correlated between both types of choices, indicating that both types of choices did not entail fundamentally different processing demands.

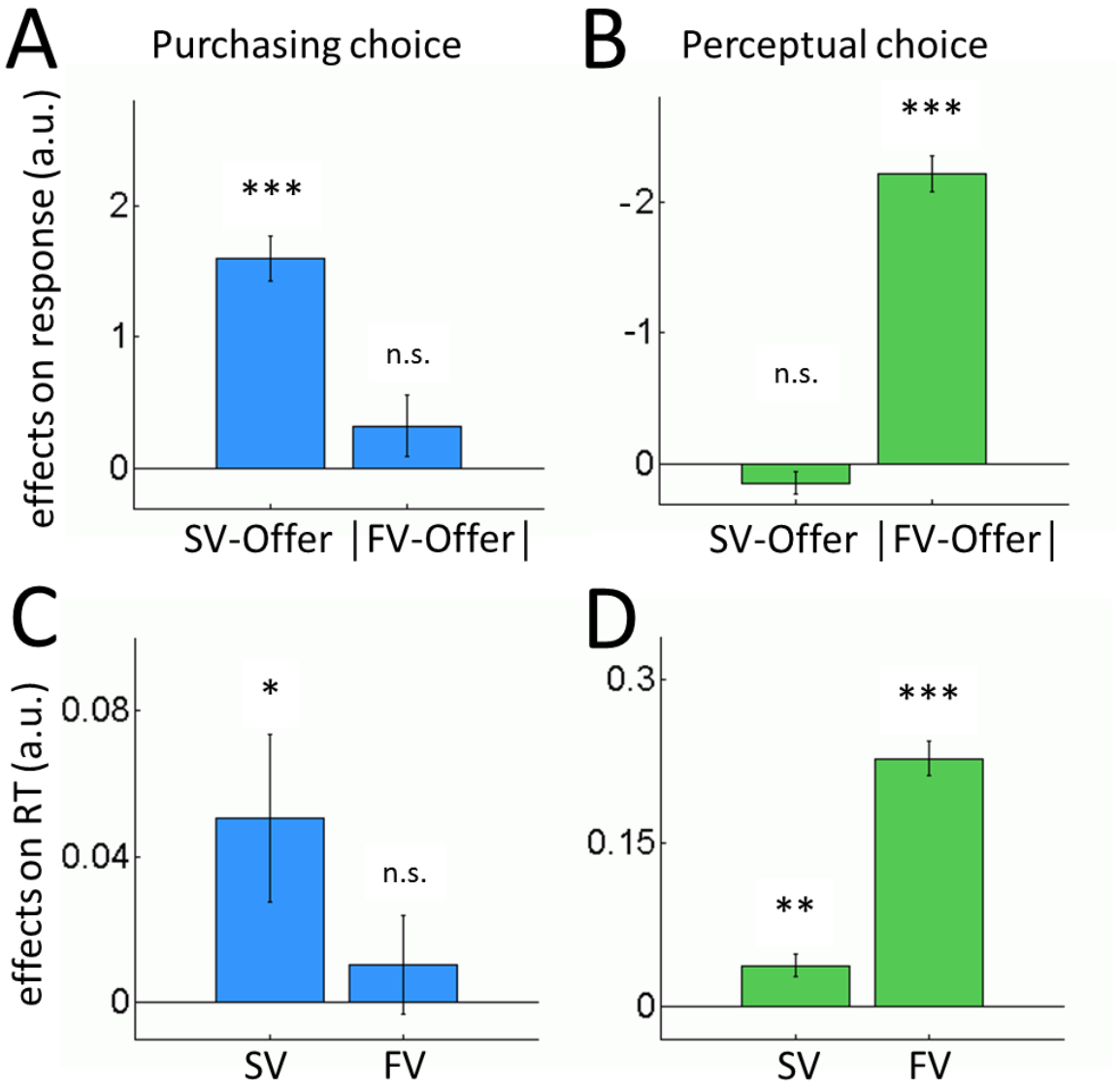

Figure 2. Behavioral results.

The trial wise SVs were directly relevant for the participant's purchasing decisions but irrelevant for the matched perceptual decisions.

(A-B) During purchasing trials, decisions to accept or reject depended positively on the difference between SV and the aurally presented price (multiple logistic regression; t_{25} = 9.24, P = 1.5*10^{-9}), while this index was irrelevant for perceptual choices (t_{25} = 1.37, P = 0.18). This regression indicates that the higher the difference between SV and offer price (consumer surplus) the more likely a purchase response.

During perceptual trials, responses depended negatively on the absolute difference between the number of faces (FV) and the aurally presented number (t_{25} = -16.03, P = 1.2*10^{-14}), while this index was irrelevant during purchasing choices (t_{25} = 1.62, P = 0.12). This regression indicates that the higher the absolute difference between FV and the offered criterion the less likely an accept response. Please note the y-scale in (B) has been inverted to facilitate illustration and visual comparison with the other panels.

(C) Reaction times during purchasing decisions were significantly affected by the task-relevant SV (t_{25} = 2.22, P = 0.036), while the number of faces on the cover had no effect (t_{25} = 0.76, P = 0.45) on RTs.

(D) RTs during perceptual choices were slowed down by task-relevant FV (t_{25} = 14.3517, P = 1.4*10^{-13}) and crucially also by task-irrelevant SV (t_{25} = 3.66, P = 0.00117), thereby confirming value-based attentional capture.

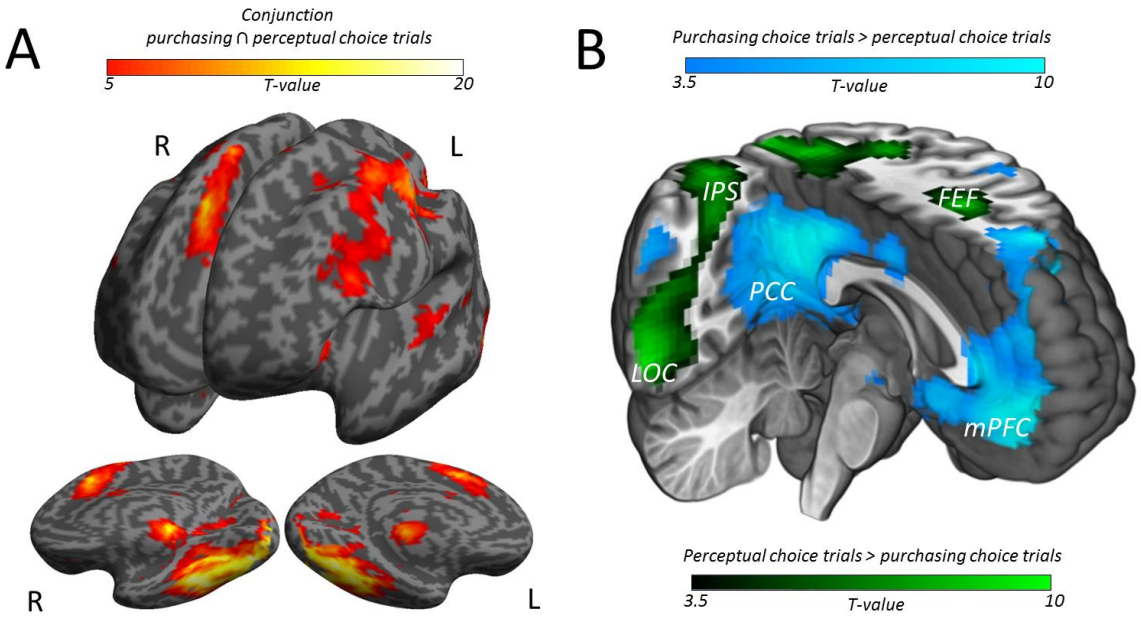

Figure 3. Average brain activity that is common and distinct for both types of choice.

(A) Common decision-related activity in both tasks (conjunction at $P < 0.05$, FWE-cluster-corrected, see **Table S1** for complete list) was found in the ventral visual stream along the fusiform gyrus, in subcortical visual areas such as the lateral geniculate nucleus, and in the auditory cortex along the bilateral superior temporal gyrus. In addition, we find regions associated with motor responses – such as the SMA, pre-SMA, and the left motor cortex - similarly engaged in both tasks. SMA = supplementary motor area.

(B) Contrasting average decision-related activity (not parametric modulation by SV) between both types of choice revealed distinct activations for purchasing and perceptual choices. Blue represents significant activity for purchasing > perceptual choices (see **Table S2**), whereas green represents significant activity for perceptual > purchasing choices (see **Table S3**) (both at $P < 0.05$, FWE-cluster-corrected).

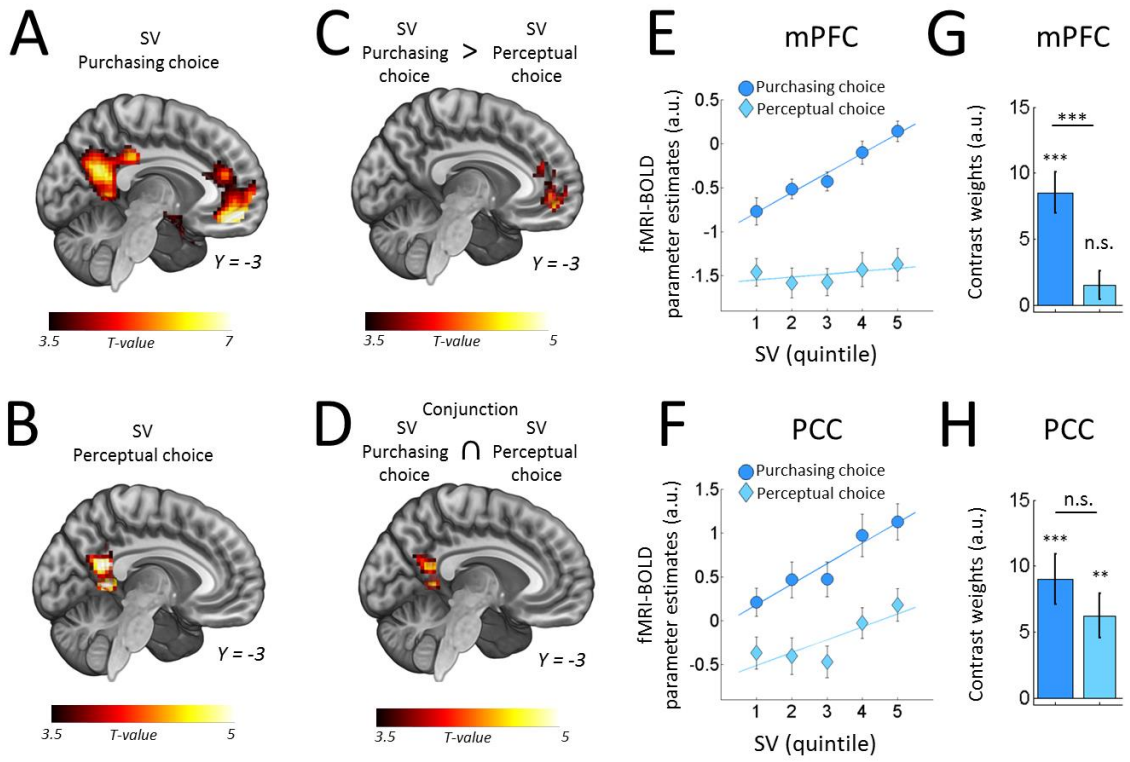

Figure 4. Distinct SV representations in mPFC and PCC.

(A) Choice-relevant SV during purchasing decisions correlates with BOLD signals in mPFC and PCC (see **Table S4** for statistics and peak coordinates and see also **Figure S1** for SV representations in the ventral striatum).

(B) Choice-irrelevant SV during perceptual decisions correlates with BOLD signals in PCC, bilateral DLPFC and bilateral parietal lobule (see **Figure S2** and **Table S5** for statistics and peak coordinates).

(C) A direct comparison of SV representations during purchasing choices versus SV representations during perceptual choices reveals a slope increase when SV is choice-relevant (during purchasing choices) in mPFC (peak t_{25} = 4.72, x = -3, y = 50, z = -11, P = 0.05, FWE-cluster-corrected). This effect is visualized in panel (E) by the parameter estimates extracted from 5-mm spheres centered on peak voxels of the choice-relevant SV > choice-irrelevant SV contrast, determined by the leave-one-

subject-out procedure to ensure independence (see **Experimental Procedures** for details).

(D) A conjunction analysis between SV representations during purchasing choices and perceptual choices reveals a task-invariant SV representation in PCC (conjunction, peak t_{25} = 5.04, x = -6, y = -52, z = 19, P < 0.05, FWE-cluster-corrected). This effect is visualized in panel (F) by the parameter estimates extracted from 5-mm spheres centered on peak voxels of the choice-irrelevant SV contrast, as determined by the leave-one-subject-out procedure.

(G) and (H) visualize and quantify the slopes of the choice-relevant (dark blue) and choice-irrelevant (light blue) SV representation in mPFC and PCC, respectively. The panels plot the contrast weights from the same 5mm spheres as in (E) and (F) respectively. BOLD activity in both mPFC (t_{25} = 5.26, p = $1.8*10^{-5}$) and PCC (t_{25} = 4.64, p = $9.4*10^{-5}$) significantly increases with increasing task-relevant SV, but only activity in PCC also significantly increases with increasing task-irrelevant SVs (t_{25} = 3.66, p = $1.2*10^{-3}$). In direct comparisons, the slope of the task-relevant SV representation in mPFC is significantly increased compared to the task-irrelevant SV representation (t_{25} = 4.30, p = $2.3*10^{-4}$), whereas no such difference could be observed for PCC (t_{25} = 1.32, p = 0.1974). Error bars in all panels represent ± 1 s.e.m. (n = 26).

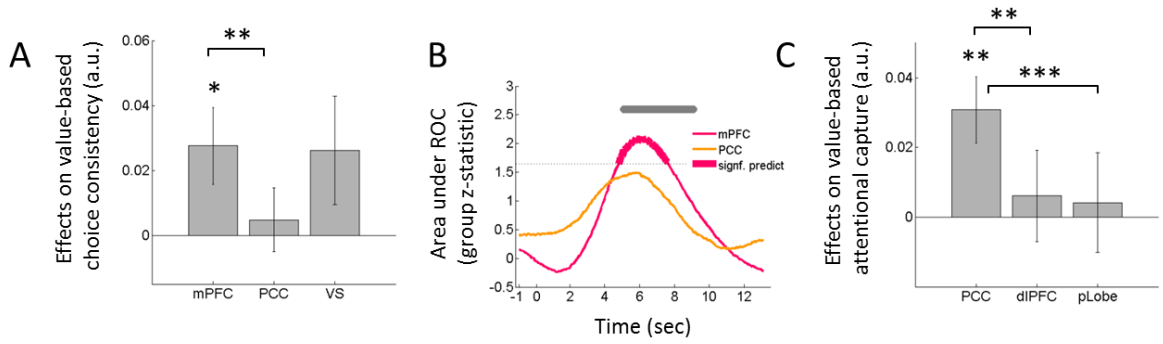

Figure 5. Relating neural activity to behavior.

(A) Value-representations in mPFC, but not PCC, relate to choice consistency. The plot shows standardized estimates from multiple regressions of choice consistency on SV-related BOLD signals in different regions. BOLD signals in mPFC (X^2 = 4.85, p = 0.027, likelihood ratio test) relate to choice consistency during purchasing decisions whereas the corresponding signals in PCC (X^2 = 0.23, p = 0.629) do not (see T**able S8**). The same analyses for the VS reveal an effect at trend level (X^2 = 2.43, p = 0.12). Importantly, the mPFC effects are significantly stronger than the corresponding effects for PCC (p = 0.01). Please see **Experimental Procedures** for details on regressions and model comparison.

(B) Neural activity in mPFC, but not PCC, can predict purchases. The plot shows the time course of purchase-predictive activity estimated as the area under the z-transformed ROC curve. BOLD signals in mPFC (red line) predict purchases significantly above chance (grey dotted horizontal line represents the one-tailed group z-statistic critical value z = 1.64) approximately 4-8 seconds after stimulus onset (thick red line), whereas PCC responses do not predict purchases at any timepoint (orange line). Additionally, mPFC signals predict participants' purchases significantly better than PCC signals during the time period indicated by the thick grey bar after stimulus onset (paired t-tests, p < = 0.05). Please see **Experimental**

Procedures for details on the ROC analysis and **Figure S3** for ventral striatum results.

(C) Value representations in PCC relate to value-driven attentional capture. The plot shows standardized estimates from multiple regressions of value-based attentional capture on value-related BOLD signals from all regions identified as showing task-irrelevant SV representations. Neural activity in PCC shows a strong relationship (X^2 = 9.83, p = $1.7*10^{-3}$) with the reaction-time slowing due to task-irrelevant SV during perceptual decisions, while dlPFC (X^2 = 0.21, p = 0.65) and parietal lobule (X^2 = 0.08, p = 0.78) do not (see T**able S9**). Please see **Experimental Procedures** for details on regressions and model comparison.

REFERENCES

Anderson, B.A. (2013). A value-driven mechanism of attentional selection. J Vis 13.

Anderson, B.A., Laurent, P.A., and Yantis, S. (2011). Value-driven attentional capture. P Natl Acad Sci USA 108, 10367-10371.

Ashburner, J., and Friston, K.J. (2005). Unified segmentation. Neuroimage 26, 839-851.

Awh, E., Belopolsky, A.V., and Theeuwes, J. (2012). Top-down versus bottom-up attentional control: a failed theoretical dichotomy. Trends Cogn Sci 16, 437-443.

Bartra, O., McGuire, J.T., and Kable, J.W. (2013). The valuation system: A coordinate-based meta-analysis of BOLD fMRI experiments examining neural correlates of subjective value. Neuroimage 76, 412-427.

Becker, G.M., Degroot, M.H., and Marschak, J. (1964). Measuring Utility by a Single-Response Sequential Method. Behav Sci 9, 226-232.

Berridge, K.C. (2012). From prediction error to incentive salience: mesolimbic computation of reward motivation. Eur J Neurosci 35, 1124-1143.

Bickel, W.K., Miller, M.L., Yi, R., Kowal, B.P., Lindquist, D.M., and Pitcock, J.A. (2007). Behavioral and neuroeconomics of drug addiction: Competing neural systems and temporal discounting processes. Drug Alcohol Depen 90, S85-S91.

Castellanos, F.X., and Proal, E. (2012). Large-scale brain systems in ADHD: beyond the prefrontal-striatal model. Trends Cogn Sci 16, 17-26.

Chau, B.K.H., Kolling, N., Hunt, L.T., Walton, M.E., and Rushworth, M.F.S. (2014). A neural mechanism underlying failure of optimal choice with multiple alternatives. Nat Neurosci 17.

Clithero, J.A., and Rangel, A. (2013). Informatic parcellation of the network involved in the computation of subjective value. Soc Cogn Affect Neurosci.

Constantinidis, C., and Procyk, E. (2004). The primate working memory networks. Cogn Affect Behav Neurosci 4, 444-465.

Corbetta, M., Miezin, F.M., Shulman, G.L., and Petersen, S.E. (1991). Selective Attention Modulates Extrastriate Visual Regions in Humans during Visual Feature Discrimination and Recognition. Ciba F Symp 163, 165-&.

Corbetta, M., and Shulman, G.L. (2002). Control of goal-directed and stimulus-driven attention in the brain. Nat Rev Neurosci 3, 201-215.

Culham, J.C., Cavanagh, P., and Kanwisher, N.G. (2001). Attention response functions: characterizing brain areas using fMRI activation during parametric variations of attentional load. Neuron 32, 737-745.

Davis, C. (2010). Attention-deficit/Hyperactivity Disorder: Associations with Overeating and Obesity. Curr Psychiat Rep 12, 389-395.

Della Libera, C., and Chelazzi, L. (2006). Visual selective attention and the effects of monetary rewards. Psychological Science 17, 222-227.

Desimone, R., and Duncan, J. (1995). Neural Mechanisms of Selective Visual-Attention. Annu Rev Neurosci 18, 193-222.

Dixon, M.R., Jacobs, E.A., and Sanders, S. (2006). Contextual control of delay discounting by pathological gamblers. J Appl Behav Anal 39, 413-422.

Eimer, M. (1996). The N2pc component as an indicator of attentional selectivity. Electroen Clin Neuro 99, 225-234.

Esterman, M., Tamber-Rosenau, B.J., Chiu, Y.C., and Yantis, S. (2010). Avoiding non-independence in fMRI data analysis: Leave one subject out. Neuroimage 50, 572-576.

Field, M., and Cox, W.M. (2008). Attentional bias in addictive behaviors: A review of its development, causes, and consequences. Drug Alcohol Depen 97, 1-20.

Friedman-Hill, S.R., Robertson, L.C., Desimone, R., and Ungerleider, L.G. (2003). Posterior parietal cortex and the filtering of distractors. P Natl Acad Sci USA 100, 4263-4268.

Glover, G.H., Li, T.Q., and Ress, D. (2000). Image-based method for retrospective correction of physiological motion effects in fMRI: RETROICOR. Magn Reson Med 44, 162-167.

Green, D.M., and Swets, J.A. (1966). Signal detection theory and psychophysics (New York ; London: Wiley).

Harvey, A.K., Pattinson, K.T.S., Brooks, J.C.W., Mayhew, S.D., Jenkinson, M., and Wise, R.G. (2008). Brainstem Functional Magnetic Resonance Imaging: Disentangling Signal From Physiological Noise. J Magn Reson Imaging 28, 1337-1344.

Hayden, B.Y., Nair, A.C., McCoy, A.N., and Platt, M.L. (2008). Posterior cingulate cortex mediates outcome-contingent allocation of behavior. Neuron 60, 19-25.

Heilbronner, S.R., and Platt, M.L. (2013). Causal Evidence of Performance Monitoring by Neurons in Posterior Cingulate Cortex during Learning. Neuron 80, 1384-1391.

Hickey, C., Chelazzi, L., and Theeuwes, J. (2011). Reward has a residual impact on target selection in visual search, but not on the suppression of distractors. Vis Cogn 19, 117-128.

Hutton, C., Josephs, O., Stadler, J., Featherstone, E., Reid, A., Speck, O., Bernarding, J., and Weiskopf, N. (2011). The impact of physiological noise correction on fMRI at 7 T. Neuroimage 57, 101-112.

Kahneman, D., and Tversky, A. (1979). Prospect Theory - Analysis of Decision under Risk. Econometrica 47, 263-291.

Kanwisher, N., and Wojciulik, E. (2000). Visual attention: insights from brain imaging. Nat Rev Neurosci 1, 91-100.

Kasper, L., Marti, S., Vannesjö, J., Hutton, C., Dolan, R., Weiskopf, N., Stephan, K.E., and Prüssmann, K.P. (2009). Cardiac Artefact Correction for Human Brainstem fMRI at 7 Tesla. In Org Hum Brain Mapping (San Francisco).

Kastner, S., Pinsk, M.A., De Weerd, P., Desimone, R., and Ungerleider, L.G. (1999). Increased activity in human visual cortex during directed attention in the absence of visual stimulation. Neuron 22, 751-761.

Katsuki, F., and Constantinidis, C. (2012). Unique and shared roles of the posterior parietal and dorsolateral prefrontal cortex in cognitive functions. Front Integr Neurosci 6, 17.

Kim, H., Adolphs, R., O'Doherty, J.P., and Shimojo, S. (2007). Temporal isolation of neural processes underlying face preference decisions. P Natl Acad Sci USA 104, 18253-18258.

Kiss, M., Driver, J., and Eimer, M. (2009). Reward priority of visual target singletons modulates event-related potential signatures of attentional selection. Psychol Sci 20, 245-251.

Knudsen, E.I. (2007). Fundamental components of attention. Annu Rev Neurosci 30, 57-78.

Knutson, B., Rick, S., Wirnmer, G.E., Prelec, D., and Loewenstein, G. (2007). Neural predictors of purchases. Neuron 53, 147-156.

Krajbich, I., Armel, C., and Rangel, A. (2010). Visual fixations and the computation and comparison of value in simple choice. Nat Neurosci 13, 1292-1298.

Krajbich, I., Lu, D.C., Camerer, C., and Rangel, A. (2012). The attentional drift-diffusion model extends to simple purchasing decisions. Front Psychol 3.

Kriegeskorte, N., Simmons, W.K., Bellgowan, P.S.F., and Baker, C.I. (2009). Circular analysis in systems neuroscience: the dangers of double dipping. Nat Neurosci 12, 535-540.

Lebreton, M., Jorge, S., Michel, V., Thirion, B., and Pessiglione, M. (2009). An Automatic Valuation System in the Human Brain: Evidence from Functional Neuroimaging. Neuron 64, 431-439.

Lennert, T., and Martinez-Trujillo, J. (2011). Strength of Response Suppression to Distracter Stimuli Determines Attentional-Filtering Performance in Primate Prefrontal Neurons. Neuron 70, 141-152.

Leotti, L.A., Iyengar, S.S., and Ochsner, K.N. (2010). Born to choose: the origins and value of the need for control. Trends Cogn Sci 14, 457-463.

Levy, I., Lazzaro, S.C., Rutledge, R.B., and Glimcher, P.W. (2011). Choice from Non-Choice: Predicting Consumer Preferences from Blood Oxygenation Level-Dependent Signals Obtained during Passive Viewing. J Neurosci 31, 118-125.

Lim, S.L., O'Doherty, J.P., and Rangel, A. (2011). The Decision Value Computations in the vmPFC and Striatum Use a Relative Value Code That is Guided by Visual Attention. J Neurosci 31, 13214-13223.

Luck, S.J., Girelli, M., McDermott, M.T., and Ford, M.A. (1997). Bridging the gap between monkey neurophysiology and human perception: An ambiguity resolution theory of visual selective attention. Cognitive Psychol 33, 64-87.

Luck, S.J., and Hillyard, S.A. (1994). Electrophysiological correlates of feature analysis during visual search. Psychophysiology 31, 291-308.

Martinez-Trujillo, J.C., and Treue, S. (2004). Feature-based attention increases the selectivity of population responses in primate visual cortex. Current Biology 14, 744-751.

Moran, J., and Desimone, R. (1985). Selective Attention Gates Visual Processing in the Extrastriate Cortex. Science 229, 782-784.

Noonan, M.P., Walton, M.E., Behrens, T.E.J., Sallet, J., Buckley, M.J., and Rushworth, M.F.S. (2010). Separate value comparison and learning mechanisms in macaque medial and lateral orbitofrontal cortex. P Natl Acad Sci USA 107, 20547-20552.

O'Connell, R.G., Dockree, P.M., and Kelly, S.P. (2012). A supramodal accumulation-to-bound signal that determines perceptual decisions in humans. Nat Neurosci 15, 1729-1735.

Padoa-Schioppa, C. (2013). Neuronal Origins of Choice Variability in Economic Decisions. Neuron 80, 1322-1336.

Pearson, J.M., Hayden, B.Y., Raghavachari, S., and Platt, M.L. (2009). Neurons in Posterior Cingulate Cortex Signal Exploratory Decisions in a Dynamic Multioption Choice Task. Current Biology 19, 1532-1537.

Pearson, J.M., Heilbronner, S.R., Barack, D.L., Hayden, B.Y., and Platt, M.L. (2011). Posterior cingulate cortex: adapting behavior to a changing world. Trends Cogn Sci 15, 143-151.

Plassmann, H., O'Doherty, J., and Rangel, A. (2007). Orbitofrontal cortex encodes willingness to pay in everyday economic transactions. J Neurosci 27, 9984-9988.

Poldrack, R.A., and Mumford, J.A. (2009). Independence in ROI analysis: where is the voodoo? Soc Cogn Affect Neur 4, 208-213.

Posse, S., Wiese, S., Gembris, D., Mathiak, K., Kessler, C., Grosse-Ruyken, M.L., Elghahwagi, B., Richards, T., Sr, D., and Kiselev, V.G. (1999). Enhancement of BOLD-contrast sensitivity by single-shot multi-echo functional MR imaging. Magn Reson Med 42, 87-97.

Rangel, A., Camerer, C., and Montague, P.R. (2008). A framework for studying the neurobiology of value-based decision making. Nat Rev Neurosci 9, 545-556.

Reddy, L., Quiroga, R.Q., Wilken, P., Koch, C., and Fried, I. (2006). A single-neuron correlate of change detection and change blindness in the human medial temporal lobe. Curr Biol 16, 2066-2072.

Reynolds, J.H., and Chelazzi, L. (2004). Attentional modulation of visual processing. Annu Rev Neurosci 27, 611-647.

Reynolds, J.H., and Heeger, D.J. (2009). The Normalization Model of Attention. Neuron 61, 168-185.

Reynolds, J.H., Pasternak, T., and Desimone, R. (2000). Attention increases sensitivity of V4 neurons. Neuron 26, 703-714.

Rieger, J.W., Gegenfurtner, K.R., Schalk, F., Koechy, N., Heinze, H.J., and Grueschow, M. (2013). BOLD responses in human V1 to local structure in natural scenes: Implications for theories of visual coding. J Vision 13.

Rolls, E.T., and Grabenhorst, F. (2008). The orbitofrontal cortex and beyond: From affect to decision-making. Prog Neurobiol 86, 216-244.

Sasson, N.J., Elison, J.T., Turner-Brown, L.M., Dichter, G.S., and Bodfish, J.W. (2011). Brief report: Circumscribed attention in young children with autism. J Autism Dev Disord 41, 242-247.

Sasson, N.J., Turner-Brown, L.M., Holtzclaw, T.N., Lam, K.S., and Bodfish, J.W. (2008). Children with autism demonstrate circumscribed attention during passive viewing of complex social and nonsocial picture arrays. Autism Res 1, 31-42.

Schmiedeskamp, H., Newbould, R.D., Pisani, L.J., Skare, S., Glover, G.H., Pruessmann, K.P., and Bammer, R. (2010). Improvements in Parallel Imaging Accelerated Functional MRI Using Multiecho Echo-Planar Imaging. Magn Reson Med 63, 959-969.

Skudlarski, P., Constable, R.T., and Gore, J.C. (1999). ROC analysis of statistical methods used in functional MRI: individual subjects. Neuroimage 9, 311-329.

Sorenson, J.A., and Wang, X. (1996). ROC methods for evaluation of fMRI techniques. Magn Reson Med 36, 737-744.

Spitzer, H., Desimone, R., and Moran, J. (1988). Increased Attention Enhances Both Behavioral and Neuronal Performance. Science 240, 338-340.

Strait, C.E., Blanchard, T.C., and Hayden, B.Y. (2014). Reward Value Comparison via Mutual Inhibition in Ventromedial Prefrontal Cortex. Neuron 82, 1357-1366.

Theeuwes, J., and Belopolsky, A.V. (2012). Reward grabs the eye: Oculomotor capture by rewarding stimuli. Vision Res 74, 80-85.

Todd, J.J., and Marois, R. (2004). Capacity limit of visual short-term memory in human posterior parietal cortex. Nature 428, 751-754.

Towal, R.B., Mormann, M., and Koch, C. (2013). Simultaneous modeling of visual saliency and value computation improves predictions of economic choice. P Natl Acad Sci USA 110, E3858-E3867.

Tusche, A., Bode, S., and Haynes, J.D. (2010). Neural Responses to Unattended Products Predict Later Consumer Choices. J Neurosci 30, 8024-8031.

Woodman, G.F., and Luck, S.J. (1999). Electrophysiological measurement of rapid shifts of attention during visual search. Nature 400, 867-869.

Supplemental Information

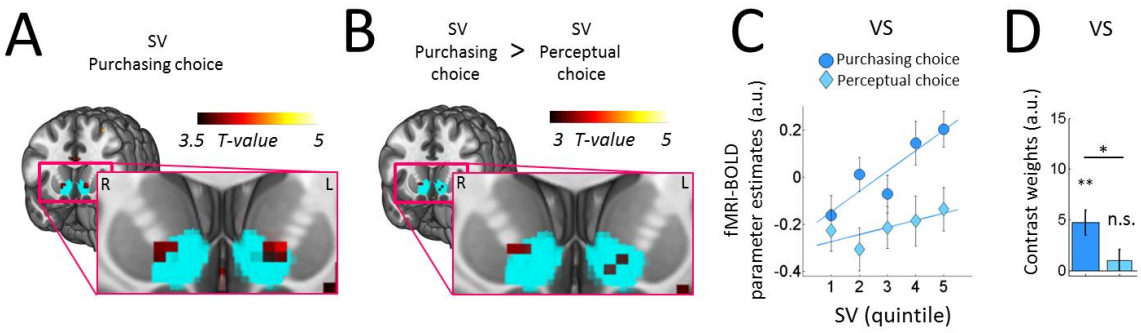

Figure S1, SV response profiles in the ventral striatum, related to Figure 4.

(A) During purchasing decisions, choice-relevant SV is represented in bilateral ventral striatum (VS_{left}, peak t_{25} = 4.12, x = -12, y = 11, z = -2, P = 0.027, VS_{right}, peak t_{25} = 4.06, x = 15, y = 11, z = -2, P = 0.042, small-volume-corrected, see **Experimental Procedures** for details).

(B) The VS shows significant sharpening of the choice-relevant SV response profile (higher slope of choice-relevant SV response profile as compared to choice-irrelevant SV response profile) (peak t_{25} = 3.4, x = 15, y = 14, z = -2, P = 0.049, small-volume-corrected), cyan shaded area corresponds to nucleus accumbens mask from FSL-Harvard-Oxford-atlas.

(C) Mean BOLD signal estimates extracted from VS as a function of choice-relevant SV during purchasing choice and choice-irrelevant, automatic SV during perceptual choice. The parameter estimates were extracted from 5-mm spheres centered on peak voxels of the choice-relevant SV contrast, as determined by the leave-one-subject-out procedure. Plot follows the same procedures and conventions as in **Figure 4E-F**. Error bars represent ± 1 s.e.m. (n = 26).

(D) The slopes of the task-relevant (dark blue) and task-irrelevant (light blue) SV representations are plotted as the contrast weights extracted from the same 5mm spheres determined by the leave-one-subject-out procedure as in (C). VS significantly (t_{25} = 3.65, p = $1.2*10^{-3}$) increases its responses with increasing task-relevant SV while no such effect is found for the task-irrelevant SV representation VS (t_{25} = 0.95, p = 0.3410). The slope of the task-relevant SV representation in VS is significantly increased compared to the task-irrelevant SV representation (t_{25} = 2.46, p = 0.02). Error bars represent ± 1 s.e.m. (n = 26).

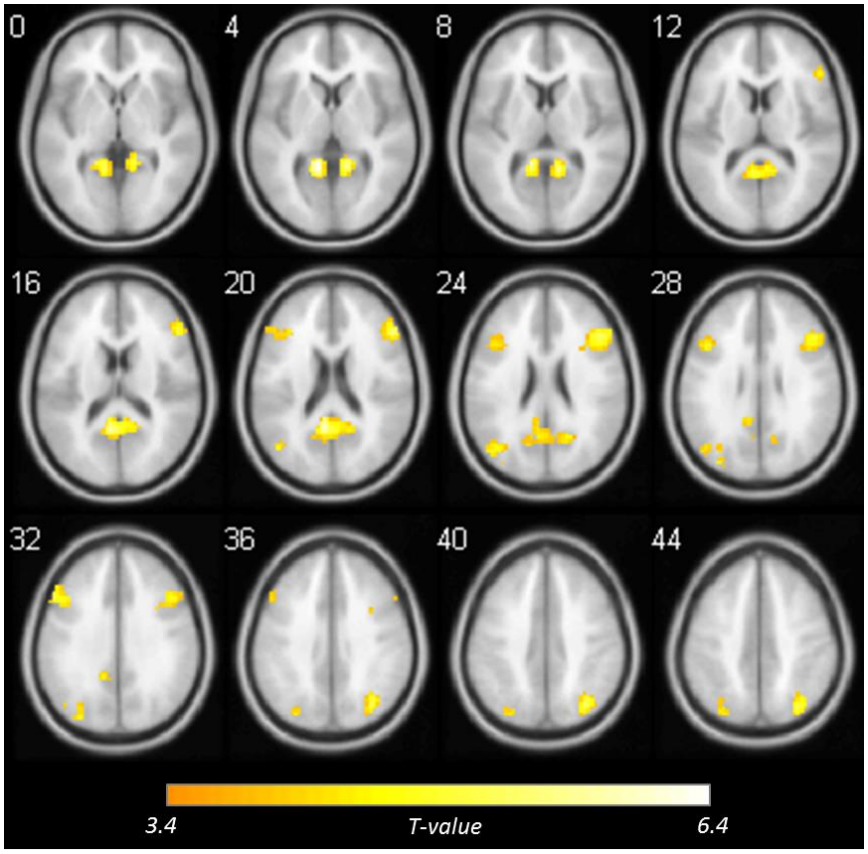

Figure S2, Choice-irrelevant SV representations during perceptual decisions, related to Figure 4B.

During perceptual choices, choice-irrelevant SV is represented in posterior cingulate cortex, bilateral dorsolateral prefrontal cortex (dlPFC, comprising BA46 & BA9 in the middle frontal gyrus) and bilateral parietal lobule (comprising BA7 and BA39 in the superior parietal Lobe and the angular gyrus) (**Table S5**). (*P* = 0.05 FWE-cluster-corrected). White numbers adjacent to each axial brain slice indicate the respective z-coordinate in MNI-space.

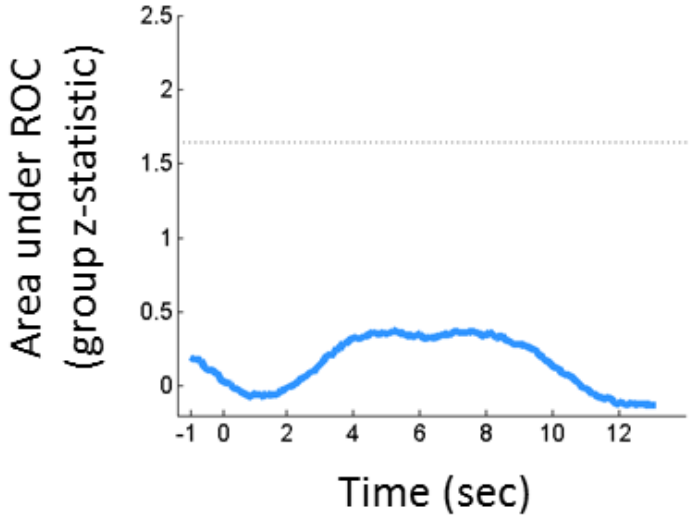

Figure S3, Ventral striatum does not predict purchases, related to Figure 5B.
The plot shows the time course of the area under the z-transformed ROC curve for the ventral striatum (VS). BOLD signals in VS (blue line) do not predict purchases significantly above chance (grey dotted horizontal line represents the one-tailed group z-statistic critical value z = 1.64). This finding is well in line with previous reports (Knutson et al., 2007) in which VS activity was also not predictive of purchasing choices when price and product were simultaneously presented as in our paradigm. Interestingly, Knutson et al. report that when the price and product are simultaneously presented, mPFC predicts purchases, which is exactly what we find in the present work and illustrate in Figure **5B** of the main text. Please see **Experimental Procedures** for details on the ROC analysis.

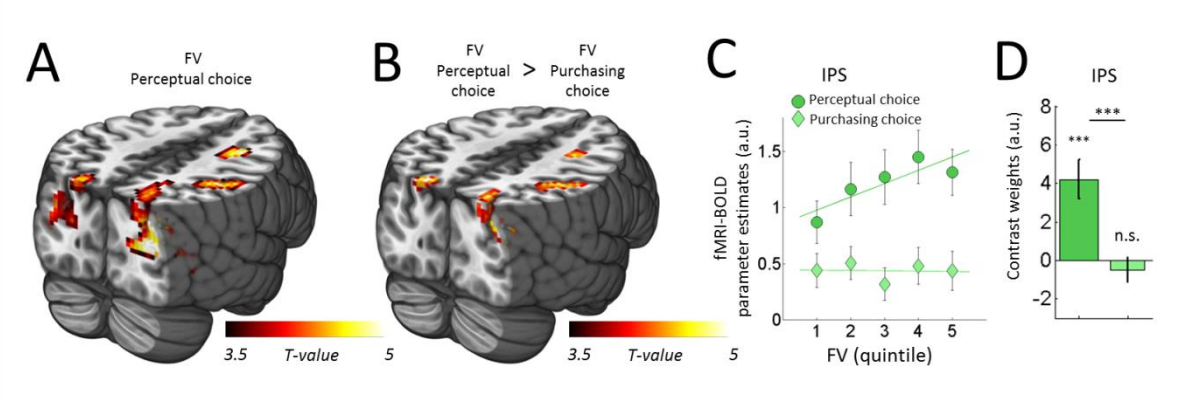

Figure S4, Perceptual response profiles in the IPS, related to Figure 4.

(A) During perceptual choices, choice-relevant FV (number of faces on the cover) is represented in IPS, FEF and LOC (IPS, peak t_{25} = 5.10, x = 18, y = -73, z = 58, FEF, peak t_{25} = 5.61, x = 30, y = 8, z = 49 and LOC, peak t_{25} = 6.13, x = 39, y = -76, z = 22; displayed at *P* = 0.05 FWE-cluster-corrected).

(B) When contrasting the slopes of choice-relevant (**Table S6**) and choice-irrelevant (**Table S7**) FV representations, significant sharpening of choice-relevant FV representations is observed in IPS and FEF (IPS, peak t_{25} = 5.08, x = 15, y = -67, z = 58, FEF, peak t_{25} = 5.57, x = 27, y = 2, z = 58, displayed at *P* = 0.05 FWE-cluster-corrected). A visualization of this effect is shown in panel (C & D)

(C) BOLD signal estimates in the IPS as a function of choice-relevant (circles) and choice-irrelevant, automatic (diamonds) FV. The parameter estimates were extracted from 5-mm spheres centered on peak voxels of the choice-relevant higher choice-irrelevant SV contrast, determined by the leave-one-subject-out procedure. Error bars represent ± 1 s.e.m. (n = 26).

(D) Visualization of the slopes in (C) of the task-relevant (dark green) and task-irrelevant (light green) SV representation by plotting the contrast weights from the same 5mm spheres determined by the leave-one-subject-out procedure as in (C). The plot follows the same conventions as in **Figure 4 E-H.** *** = p < 0.001, Error bars represent ± 1 s.e.m. (n = 26).

Supplemental Tables

Supplemental Table S1, Regions activated during both types of decisions (conjunction between purchasing and perceptual choice trials), related to Figure 3A.

Region	Peak-Side	Cluster Size	x	y	z	Z score	T score	p-value
Fusiform gyrus	L	6462	-36	-76	-11	Inf	20.06	<0.001
Front. sup. med.	R	850	6	20	43	Inf	14.69	<0.001
Insula	L	185	-30	26	1	7.80	11.02	<0.001
Insula	R	233	36	17	7	7.54	10.37	<0.001
Inf. front. sulcus	R	167	42	8	28	6.54	8.29	<0.001
Sup. temp. gyrus	L	117	-63	-10	1	5.95	7.22	<0.001
Sup. temp. gyrus	R	81	66	-10	1	5.87	7.09	<0.001
LGN	R	410	21	-28	-5	Inf	13.45	<0.001
Sup. Colliculi	R	410	6	-28	-2	Inf	15.04	<0.001

All p-values are FWE-corrected for the whole brain. Front. = frontal, Sup. = superior, temp. = temporal. Med. = medial, Inf. = inferior. LGN = lateral geniculate nucleus. Coordinates are listed in MNI space

Supplemental Table S2, Regions activated more strongly during purchasing than during perceptual choice trials, related to Figure 3B.

Region	Peak-Side	Cluster Size	x	y	z	Z score	T score	p-value
mPFC	L	637	-3	47	-8	7.32	14.02	<0.001
PCC	R	584	0	-52	25	6.94	12.32	<0.001
Sup. temp. gyrus	L	390	-57	-22	1	6.57	10.96	<0.001
Sup. temp. gyrus	R	313	63	-7	-5	6.13	9.50	<0.001
Sup. Front.	L	243	-21	41	43	6.48	10.64	<0.001
Hippocampus	L	89	-27	-22	-14	5.81	8.60	<0.001
Angular gyrus	L	45	-45	-67	34	5.47	7.72	<0.001
Basal forebrain	L	42	-6	17	-14	5.14	6.96	<0.001
Inf. front. gyrus	L	34	-36	26	-14	6.14	9.55	<0.001

All p-values are FWE-corrected for the whole brain. mPFC = medial prefrontal cortex, PCC = posterior cingulate cortex, Front. = frontal, Sup. = superior, temp. = temporal. Med. = medial, Inf. = inferior. Coordinates are listed in MNI space.

Supplemental Table S3, Regions activated more strongly during perceptual than during purchasing choice trials, related to Figure 3B.

Region	Peak-Side	Cluster Size	x	y	z	Z score	T score	p-value
Inf. temp. gyrus	R	830	51	-55	-8	6.47	10.60	<0.001
Ant. par. Sulcus	R	173	33	-43	40	6.31	10.07	<0.001
IPS	L	222	-18	-67	58	6.09	9.40	<0.001
FEF	L	48	-21	2	49	6.06	9.30	<0.001
Inf. temp. gyrus	L	186	-36	-61	7	5.84	10.64	<0.001
Ant. par. Sulcus	L	66	-36	-49	49	5.59	8.30	<0.001
FEF	R	49	30	5	52	5.47	7.72	<0.001
Parahippocampus	L	1	-33	-43	-8	4.73	6.96	0.023

All p-values are FWE-corrected for the whole brain. IPS = Inferior parietal sulcus, FEF = Frontal eye fields, Front. = frontal, Sup. = superior, temp. = temporal. Med. = medial, Inf. = inferior. Coordinates are listed in MNI space.

Supplemental Table S4, Regions where BOLD activity was positively correlated with choice-relevant SV during purchasing decisions, related to Figure 4A.

Region	Peak-Side	Cluster Size	x	y	z	Z score	T score	p-value
mPFC	L	695	-6	50	-14	5.48	7.74	<0.001
PCC	L	997	-6	-58	25	5.02	6.70	<0.001
Parietal lobule	L	201	-45	-73	34	5.26	7.22	0.001
Parahippocampus	L	108	-30	-37	-14	4.04	4.86	0.014
Sup. frontal sulcus	L	87	-24	32	52	4.12	5.00	0.032
Sup. temp. gyrus	R	584	66	-10	1	5.15	6.97	<0.001
Sup. temp. gyrus	L	879	-66	-13	1	5.87	8.75	<0.001
Ventral striatum	L	10	-12	11	-2	3.57	4.12	0.027^{SVC}
Ventral striatum	R	5	15	11	-2	3.34	4.06	0.042^{SVC}

All p-values are cluster-level FWE-corrected for the whole brain, except when noted ^{SVC}, which indicates small-volume-correction using nucleus accumbens mask from FSL-Harvard-Oxford-atlas. mPFC = medial prefrontal cortex, PCC = posterior cingulate cortex, Sup. = superior, temp. = temporal. Coordinates are listed in MNI space.

Supplemental Table S5, Regions where BOLD activity was positively correlated with choice-irrelevant SV during perceptual decisions, related to Figure 4B.

Region	Peak-Side	Cluster Size	x	y	z	Z score	T score	p-value
PCC	L	417	-12	-49	4	4.8	6.24	<0.001
DLPFC	R	210	51	26	19	4.35	5.40	<0.001
DLPFC	L	119	-54	20	34	4.13	5.02	0.006
Parietal lobule	L	134	-39	-70	22	4.2	5.13	0.004
Parietal lobule	R	90	33	-70	40	4.16	5.07	0.020

All p-values are cluster-level FWE-corrected for the whole brain. PCC = posterior cingulate cortex, DLPFC = dorsolateral prefrontal cortex. Coordinates are listed in MNI space.

Supplemental Table S6, Regions where BOLD activity was positively correlated with choice-relevant FV during perceptual decisions, related to Figure S4A.

Region	Peak-Side	Cluster Size	x	y	z	Z score	T score	p-value
IPS	R	120	18	-73	58	4.19	5.10	0.007
FEF	R	157	30	8	49	4.47	5.61	0.002
LOC	R	612	39	-76	22	4.74	6.13	<0.001
LOC	L	85	-48	-73	10	3.84	5.13	0.028

All p-values are cluster-level FWE-corrected for the whole brain. IPS = Inferior parietal sulcus, FEF = Frontal eye fields, LOC = Lateral occipital complex. Coordinates are listed in MNI space.

Supplemental Table S7, Regions where BOLD activity was positively correlated with choice-irrelevant FV during purchasing decisions, related to Figure S4.

Region	Peak-Side	Cluster Size	x	y	z	Z score	T score	p-value
FFA	R	131	39	-46	-20	4.95	6.54	0.002
LOC	R	76	51	-70	1	4.06	4.89	0.023

All p-values are cluster-level FWE-corrected for the whole brain. FFA = Fusiform face area, LOC = Lateral occipital complex. Coordinates are listed in MNI space.

Supplemental Table S8, Linear mixed-effects model regressing SV consistency of purchasing decisions to BOLD signals representing choice-relevant SV, related to Figure 5A.

Full vs. null model						
	Df	AIC	BIC	logLik	Chi sq	P value
Intercept only						
Null-Model	3	-215.85	-207.25	110.92		
mPFC						
Full-Model	4	-218.70	-207.23	113.35	4.85	0.0276
VS						
Full-Model	4	-216.28	-204.81	112.14	2.43	0.1187
PCC						
Full-Model	4	-214.08	-202.61	111.04	0.23	0.6286
Full vs. reduced models						
mPFC vs PCC						
Reduced-Model	4	-214.08	-202.61	111.04		
Full-Model	5	-218.58	-204.24	114.29	6.49	0.0108
VS vs PCC						
Reduced-Model	4	-214.08	-202.61	111.04		
Full-Model	5	-214.44	-200.11	112.22	2.36	0.1244

Table S8. To test whether value-related BOLD response profiles relate to value-based choice consistency, we performed linear mixed-effects analyses to regress observed consistency (percent consistent) for each subject and SV quintile on the corresponding BOLD responses extracted from the three regions of interest (see **Experimental Procedures**). In all regressions, the regions were treated as fixed effects and the intercepts for each participant as random effects. To establish the relation between consistency and BOLD signals in each region, we performed likelihood ratio tests of full models containing activity in a region as regressor against the null model containing only the intercepts. This revealed significant prediction of consistency only for the mPFC but not the PCC; the VS fell just short of statistical significance (see “Full vs. null model”). Additionally, we tested for differences in the predictive power of BOLD signals in each region with a likelihood ratio test of the full

model including PCC and mPFC or VS against the reduced model including only the PCC (intercepts were included in all models). This revealed significant improvements in explaining accuracy with the BOLD signals extracted from the mPFC relative to those from the PCC region while the test comparing VS and PCC again fell just short of statistical significance.

Supplemental Table S9, Linear mixed-effects model regressing value-based attentional capture during perceptual decisions on BOLD signals representing choice-irrelevant SVs, related to Figure 5C.

Full vs. null model						
	Df	AIC	BIC	logLik	Chi sq	P value
Intercept only						
Null-Model	3	-236.37	-227.77	121.18		
PCC						
Full-Model	4	-244.19	-232.72	126.10	9.83	0.0017
DLPFC						
Full-Model	4	-234.58	-223.11	121.29	0.21	0.65
Parietal Lobule						
Full-Model	4	-234.45	-222.98	121.22	0.08	0.78
Full vs. reduced models						
PCC vs. DLPFC						
Reduced-Model	4	-234.58	-223.11	121.29		
Full-Model	5	-242.85	-228.51	126.43	10.27	0.0013
PCC vs. Parietal Lobule						
Reduced-Model	4	-234.45	-222.98	121.22		
Full-Model	5	-243.90	-229.56	126.95	11.45	0.0007
PCC vs. mPFC						
Reduced-Model	4	-238.88	-227.41	123.44		
Full-Model	5	-242.62	-228.28	126.31	5.74	0.017
PCC vs. VS						
Reduced-Model	4	-235.13	-223.66	121.56		
Full-Model	5	-242.21	-227.87	126.10	9.08	0.003

Table S9. To test whether choice-irrelevant SV BOLD response profiles relate to reaction times (RTs) for perceptual choices (i.e., whether they relate to value-based attentional capture), we performed linear mixed-effects analyses to regress observed reaction times for each subject and SV quintile on the corresponding BOLD responses extracted from the three regions showing significant choice-irrelevant SV responses (see **Table S5**). In all regressions, regions were treated as fixed effects and the intercepts for each participant as random effects. To establish the relation between RTs and BOLD signals in each region, we performed likelihood ratio tests of full models containing a region as regressor against the null model containing only the intercepts. This revealed significant prediction of RTs only for the PCC, but not the dlPFC and parietal lobule (see "Full vs. null model"). Additionally, we tested for differences in the predictive power of BOLD signals in each region with a likelihood ratio test of the full model with two regions (including PCC) against the reduced model including only the dlPFC or parietal lobule. For completeness, we also performed this test for comparisons of the PCC and the mPFC and VS, even thought the latter regions did not contain any significant SV representations during perceptual choices. Intercepts were included in all models. These comparisons revealed significant improvements in explaining RTs with the BOLD signals extracted from the PCC over those in the dlPFC, parietal lobule, mPFC and VS.

Supplemental results

Recent studies (FitzGerald et al., 2009; Jocham et al., 2012) have reported value signals in the prefrontal cortex and PCC that essentially reflect a representations of the costs associated with a given choice option. It is thus a possibility that the observed regional differences in coding choice-relevant and choice-irrelevant SV may be differentially expressed during trials in which the aurally presented price was either below or above the participants SV for each item. To confirm that the effects are indeed driven by SV and not the price level with respect to SV, we set up an additional GLM identical to the main model (see **Experimental Procedures** for details) but crucially the indicator functions were separately assigned to trials were the price was below or above the SV. We found that the choice-relevant SV > choice-irrelevant SV contrast maps did not differ between for trials with either prices higher or lower than the SV, even at an extremely liberal uncorrected threshold of $p < 0.005$. In a similar vein, we did not find any significant differences when comparing the effect size of the choice-relevant > choice-irrelevant SV contrast between the two groups of trials in region-of-interest (ROI) analyses for the three BVS regions (mPFC: $t_{25} = 1.53$, $p = 0.14$, PCC: $t_{25} = 0.75$, $p = 0.46$, VS: $t_{25} = 1.3$, $p = 0.21$; see **Experimental Procedures** for details). These control analyses therefore confirm that the SV response enhancement during purchasing choices was independent of the offered price level, at least for the value ranges employed in this study.

Moreover, to confirm that SV and not price is the main determinant of brain activity in the BVS during purchasing choices, we further explored whether the aurally presented price would explain any additional variance in the brain valuation system, on top of that explained by SV. The main GLM (see **Experimental Procedures** for details) contained additional parametric regressors for price (which was orthogonalized with respect to SV) for each subject. When testing these contrasts for significance by one-sample *t* tests across the whole brain, we found no brain regions other than the auditory cortex that showed correlations of BOLD signal with the variance uniquely explained by price level, even at an uncorrected threshold of $p < 0.005$. Note that auditory cortex can be expected to correlate with the aurally presented prices, which provide more elaborate auditory input for higher price levels. In a related control analysis, we repeated the same procedure but now modeled the difference between value and price. Again, even at a relaxed uncorrected threshold of $p < 0.005$, there were no significant effects of value-price difference on BOLD

activity in BVS regions. Thus, the SV of the choice option was the primary driver of BOLD activity in the mPFC and VS during purchasing trials, and the mechanism that enhances these value representations when the choice depends on SV operates independently of the price or price-value difference.

Supplemental References

FitzGerald, T.H.B., Seymour, B., and Dolan, R.J. (2009). The Role of Human Orbitofrontal Cortex in Value Comparison for Incommensurable Objects. J Neurosci 29, 8388-8395.

Jocham, G., Hunt, L.T., Near, J., and Behrens, T.E.J. (2012). A mechanism for value-guided choice based on the excitation-inhibition balance in prefrontal cortex. Nat Neurosci 15, 960-961.

Knutson, B., Rick, S., Wirnmer, G.E., Prelec, D., and Loewenstein, G. (2007). Neural predictors of purchases. Neuron 53, 147-156.